Journal of Drug Delivery Science and Technology 74 (2022) 103606

Contents lists available at ScienceDirect

Journal of Drug Delivery Science and Technology

journal homepage: www.elsevier.com/locate/jddst

A low-intensity repetitive transcranial magnetic stimulation coupled to magnetic nanoparticles loaded with scutellarin enhances brain protection against cerebral ischemia reperfusion injury

Libin Wang [a,b,1], Shanshan Yang [b,c,1], Lisu Li [a,b], Yong Huang [a,c], Ruixi Li [a,c], Shumei Fang [a,c], Jincheng Jing [a,c], Chang Yang [a,c,*]

[a] State Key Laboratory of Functions and Applications of Medicinal Plants/Guizhou Provincial Key Laboratory of Pharmaceutics, Guizhou Medical University, Guiyang, 550004, Guizhou, China
[b] School of Pharmacy, Guizhou Medical University, Guiyang, 550004, Guizhou, China
[c] Engineering Research Center for the Development and Application of Ethnic Medicine and TCM (Ministry of Education), Guizhou Medical University, Guiyang, 550004, Guizhou, China

ARTICLE INFO

Keywords:
Stroke
Cerebral ischemia
Repetitive transcranial magnetic stimulation
Magnetic nanoparticles
Scutellarin
Alternating magnetic field

ABSTRACT

It is reported here that a portable repetitive transcranial magnetic stimulation device with low intensity (LI-rTMS, 6–9 mT) combination with magnetic nanoparticles loaded with scutellarin (SCU MNPs), a flavone extracted from the Chinese herbal medicine Erigeron breviscapus (Vant.) Hand.-Mazz, can enhance the brain protection of SCU against cerebral ischemia/reperfusion (I/R) injury of rats. To establish the focal cerebral I/R injury model, the middle cerebral artery (MCA) of male Sprague-Dawley (SD) rats was occluded for 1 h. A prolonged blood circulation was observed in our SCU MNPs in rats with cerebral ischemia. More importantly, the accumulation of SCU in brain tissue caused by LI-rTMS during SCU MNPs treatment can significantly reduce the amount of cerebral infarct after cerebral I/R compared to free SCU or SCU MNPs alone. H&E and TUNEL staining also revealed that the combined use of SCU MNPs and LI-rTMS improved neuronal architecture and morphology, and reduced apoptosis in the brain, respectively. Results from SOD, MDA, TNF-α and IL-6 tests further confirm that LI-rTMS coupled with SCU MNPs can be synergistic in treating cerebral I/R injuries through anti-oxidant and anti-inflammatory pathways. As a result, our injectable SCU MNPs combined with LI-rTMS provide promising protection against brain damage caused by cerebral I/R, and the combination of magnetic nanoparticles with LI-rTMS may also be useful as a potential drug delivery system for brain diseases.

1. Introduction

In the world, stroke is the second leading cause of death and contributes significantly to disability [1,2]. According to the 2016 Global Burden of Disease Study, China had the highest estimated lifetime stroke risk of up to 39.3% from age 25 years onwards, higher than Western Europe's 22.2% and North America's 22.4% [3]. Ischemic stroke begins when blood flow to parts of the brain is blocked or reduced, resulting in cell death if reperfusion is not occurred within a short period of time [4]. Unfortunately, the only approved treatment options for patients are mechanical thrombectomy and thrombolysis through tPA administration [5,6]. In light of the lack of available options, novel methods are necessary to minimize or reverse the damage caused by ischemic stroke.

Transcranial magnetic stimulation (TMS) is an indirect and non-invasive method that has gained a lot of attention recently. Induction of excitability changes in the motor cortex is possible by means of generating a magnetic field that passes through the scalp [7]. Generally, single-pulse TMS (including paired-pulse TMS) is used to investigate brain function [8], while repetitive TMS (rTMS) is used to cause lasting changes in brain activity [9]. Thus, rTMS appears to be a potential

Abbreviations: SCU, Scutellarin; LI-rTMS, Low intensity-repetitive transcranial magnetic stimulation; MNPs, Magnetic nanoparticles; AMF, Alternating magnetic field; SMF, Static magnetic field; I/R, Ischemia/Reperfusion; PLGA, poly(lactic-co-glycolic acid); MCAO, Middle cerebral artery occlusion.

* Corresponding author. State Key Laboratory of Functions and Applications of Medicinal Plants/Guizhou Provincial Key Laboratory of Pharmaceutics, Guizhou Medical University, No.4 Beijing Road, Guiyang, 550004, China.
E-mail address: clare_yangchang@163.com (C. Yang).
[1] These authors contributed equally to this work.

https://doi.org/10.1016/j.jddst.2022.103606
Received 20 June 2022; Received in revised form 11 July 2022; Accepted 14 July 2022
Available online 19 July 2022
1773-2247/

therapy for neurological and psychiatric diseases, such as neuropathic pain [10], stroke [11], and others. In general, rTMS is a safe practice [12]. The majority of the adverse effects were mild, with headache or dizziness being most common [13]. But the most serious safety hazard of TMS is its potential to cause noise-induced hearing loss or seizures [12,14]. Thus, we consider the combination of low intensity-repetitive transcranial magnetic stimulation (LI-rTMS) devices with chemotherapy to treat ischemic stroke.

In our previous studies [15], it is found that scutellarin (SCU, 4,5,6-trihydroxyflavone-7-glucuronide, CAS 27740-01-8), a flavonoid drug derived from the Chinese herb Erigeron breviscapus (Vant.) Hand-Mazz, can effectively reduce the cerebral infarct area and attenuate the cell apoptosis in brain tissue and protect brain against cerebral ischemia. However, SCU has a low solubility in water (0.02 mg/mL) [16]. In addition, it has a short biological half-life and poor stability (0.7h [17] - 2.3h [18]). After our encapsulation of the poly(lactic-co-glycolic acid) (PLGA) polymer, the stability of SCU was improved and the circulation time in the blood was prolonged [19]. As a result, we try to entrap the magnetic nanoparticles (Fe_3O_4 NPs) into SCU PLGA NPs and design the magnetic drug delivery system combined with LI-rTMS for the ischemic stroke.

In this study, SCU MNPs were prepared. The effect of intensity and irradiation time of alternating magnetic field (AMF) from LI-rTMS device and the effect of iron addition in the formulation on the SCU level in the brain were investigated by a UPLC-ESI-MS/MS method. The final formulation for the animal studies was optimized by Box-Behnken experimental design (see the supplementary materials). A rat model with transient middle cerebral artery occlusion (MCAO) was used to investigate the pharmacokinetic and pharmacodynamic effects of SCU MNPs combined with LI-rTMS. A series of neurological function test and histopathological examinations were carried out to confirm the superior protective activity of SCU MNPs combination with the exposure of LI-rTMS against ischemia/reperfusion (I/R) injury compared to free SCU or SCU MNPs alone.

2. Materials and methods

2.1. Materials

Oleic acid (OA)-coated Fe_3O_4 nanoparticles (particle size: ~10 nm, saturation magnetization: ~75 emu/g Fe) was obtained from Nanjing XFNANO Materials Tech Co., Ltd (Jiangsu, China). SCU (purity >98%, CAS: 27740-01-8) was purchased by Laizhang Pharmaceutical Technology Co., Ltd. (Kunming, China). Poly(vinyl alcohol) (PVA, Mw 13,000–23,000, 87–89% hydrolysed), poly(ethylene glycol) methyl ether-block-poly(lactide-co-glycolide) (PEG-PLGA, PEG average Mn 2000, PLGA average Mn 11,500), and 2,3,5-triphenyltetrazolium chloride (TTC) were obtained from Sigma Aldrich (St. Louis, USA). An acid terminated 50:50 DL-lactide/glycolide copolymer (PLGA, 0.2 dl/g, mol. wt. 17,000 g/mol) was supplied from Corbion (Gorinchem, The Netherlands). Fe standard solution was purchased from Guobiao Testing & Certification Co., Ltd. (Beijing, China). Methanol (HPLC grade) and acetonitrile (HPLC grade) were supplied from TEDIA@ High Purity Solvents (Shanghai, China). PBS solution (pH 7.4), dialysis bag (MWCO = 8,000–14,000 Da) and dialysis bag (MWCO = 30 KDa) were purchased from Solarbio® Life Sciences (Beijing, China). Paraformaldehyde, Hematoxylin-eosin staining kit (HE), 4′,6-diamidino-2-phenylindole (DAPI) and TUNEL apoptosis assay kit was obtained from Wuhan Servicebio Technology Co., Ltd. (Hubei, China). SOD, MDA and NO kits were purchased from Nanjing Jiancheng Bioengineering Institute (Nanjing, China). TNF-α and IL-6 kits were purchased from Shanghai Zhuocai Biotechnology Co., Ltd (Shanghai, China). All experiments were conducted with ultrapure water.

2.2. Preparation of SCU MNPs by nanoprecipitation

Nanoprecipitation method [19,20] was used to prepare SCU MNPs and the final formulation was optimized by Box-Behnken design (see supplementary materials). In brief, 6.4 mg SCU and 113.6 μg OA-coated Fe_3O_4 nanoparticles were dispersed in 1.5 mL methanol for 10 min under ultrasonication (250W) at room temperature. A 3 mL acetonitrile solution containing 12 mg PEG-PLGA polymers and 8 mg PLGA polymers was mixed with the SCU and Fe_3O_4 NPs methanol solution as the organic phase. A syringe was used to continuously inject the organic phase into the aqueous phase containing 3.6% (w/v) PVA while stirring continuously. After mechanical stirring for 4 h, the nanosuspension was purified in the dialysis membrane with 8,000–14,000 Da MWCO overnight at room temperature.

2.3. Nanoparticle characterization

A Nanobrook 90Plus PALS particle size analyser (Brookhaven Instruments, New York, USA) was used to measure the mean particle size, polydispersity index (PDI) and ζ potential of SCU MNPs. The samples were diluted (1:50) in ultrapure water and transferred to a polystyrene cuvette before size measurements were performed. The surface charge was measured by diluting samples with a solution of 10 mM sodium chloride (1:50). Measurements were taken in triplicate at 25 °C to determine particle size and surface charge, and the results were reported as their mean values ± standard deviation (SD).

To observe the structure and morphology of SCU MNPs, a JEOL JEM-1400 Plus transmission electron microscopy (TEM) was used. Before loading the microscope, the nanoparticle dispersions were dried in the air at room temperature after dropping on a copper grid coated with carbon.

UV–Vis spectrophotometer (UV–2401PC, Shimadzu, Japan) and Fourier transformed infrared spectroscopy (FTIR, IRTracer-100, Shimadzu, Japan) were used for composition analysis of SCU MNPs. For UV–Vis measurements, SCU, MNPs and SCU MNPs were diluted with ultrapure water (1:8) then put into the quartz cuvette and scanned from 190 nm to 800 nm. For FTIR measurements, 10 mL of obtained MNPs and SCU MNPs were concentrated to a film by rotary evaporation under a reduced pressure. The films were scanned from 4000 cm^{-1}–400 cm^{-1}.

In-vitro magnetic recruitment of SCU MNPs was tested in the presence of an external NdFeB magnet (shape: cylindrical, diameter: 2.5 cm, thickness: 0.25 cm, 0.2 T, Ningbo Lianghao Magnetic Industry Co., Ltd) compared with SCU MNPs suspension in the absence of the external magnet.

2.4. Iron analysis by atomic absorption spectrophotometer

After purification by a dialysis bag (MWCO = 30 KDa, Solarbio® Life Sciences Co. Ltd), the obtained SCU MNPs were digested with concentrated nitric acid (65%–68% w/w) at 80 °C for 4 h. The dry residue was diluted with water. The measurements of iron were carried out using a PerkinElmer PinAAcle 900T atomic absorption spectrophotometer equipped with an iron hollow cathode lamp. The following equations were used to calculate the iron encapsulation efficiency (EE) and iron loading (IL).

$$EE(\%) = \frac{M_{loaded\ Fe}}{M_{total\ Fe}} \times 100\% \quad (1)$$

$$IL(\%) = \frac{M_{loaded\ Fe}}{M_{PLGA} + M_{PVA} + M_{loaded\ SCU} + M_{loaded\ Fe}} \times 100\% \quad (2)$$

where $M_{total\ Fe}$ represented the total iron content added in the formulation before dialysis; $M_{loaded\ Fe}$ or $M_{loaded\ SCU}$ represented the iron or SCU content loaded in the nanoparticles after dialysis; M_{PLGA} represented the total amount of PEG-PLGA and PLGA polymer added; M_{PVA}

represented the total amount of PVA added.

2.5. SCU MNPs encapsulation efficiency and drug-loading

SCU MNPs were diluted with methanol (1:9 v/v) to release the free SCU and dialyzed using a dialysis membrane with 8,000–14,000 Da MWCO. An UltiMate 3000 high-performance liquid chromatography (ThermoFisher Scientific, Germering, Germany) coupled with a ZORBAX Eclipse XDB C18 column (Agilent Technologies, 4.6 × 150 mm, 5 μm) was used to determine the SCU concentration in the samples. The HPLC method was described in the literature [19]. The equations for calculating encapsulation efficiency (EE) and drug loading (DL) of SCU in SCU MNPs were shown below.

$$EE(\%) = \frac{M_{loaded\ SCU}}{M_{total\ SCU}} \times 100\% \quad (3)$$

$$DL(\%) = \frac{M_{loaded\ SCU}}{M_{PLGA} + M_{PVA} + M_{loaded\ SCU} + M_{loaded\ Fe}} \times 100\% \quad (4)$$

where $M_{total\ SCU}$ represented the total SCU content before dialysis added in the formulation; $M_{loaded\ SCU}$ or $M_{loaded\ Fe}$ represented the SCU or iron content loaded in the nanoparticles after dialysis; M_{PLGA} represented the total amount of PEG-PLGA and PLGA polymer added; M_{PVA} represented the total amount of PVA content added.

2.6. The stability of SCU MNPs

SCU MNPs were stored in a transparent glass vial at 4 °C or room temperature for one month. The particle size of SCU MNPs at 1 d, 3 d, 7 d, 14 d, and 30 d was measured by the Nanobrook 90Plus PALS particle size analyser (Brookhaven Instruments, New York, USA), and the SCU DL% of SCU MNPs was analysed by the HPLC method [19].

2.7. In vitro drug release study of nanoparticles

In vitro drug release of SCU MNPs was investigated by a dialysis method [19]. Specifically, 1.5 mL of SCU or SCU MNPs solution was placed in a dialysis bag with 8,000–14,000 Da MWCO, and the dialysis bag was then immersed in 30 mL of PBS solution (pH 7.4) containing 2 mg/mL of EDTA-2Na. The release studies were performed in a water bath with shaking (100 rpm) at a constant temperature (37 °C). 1 mL of the release medium was removed at predetermined time intervals (0.5 h, 1 h, 2 h, 4 h, 6 h, 8 h, 10 h, 12 h, and 24 h), and the same volume of medium at 37 °C was added each time. The amount of SCU in each sample was determined by HPLC measurement at 335 nm [19].

2.8. Release kinetics

For the study of the mechanism of release of SCU MNPs, data obtained from *in-vitro* release studies were fitted to the following kinetic models: zero order, first order, Higuchi, Hixson-Crowell, and Korsmeyer-Peppas.

Zero order model: $M_t/M_\infty = kt$ (5)

First order model: $M_t/M_\infty = 1\text{-}e^{-kt}$ (6)

Higuchi model: $M_t/M_\infty = kt^{1/2}$ (7)

Hixson-Crowell model: $M_t/M_\infty = k_1t + k_2t^2 + k_3t^3$ (8)

Korsmeyer-Peppas model: $M_t/M_\infty = kt^n$ (9)

Where M_t/M_∞ indicated a fraction of SCU released in time t, k indicated the rate constant, and n indicated the exponent of drug release (an indicative of drug release mechanism). *In vitro* drug release data were plotted as cumulative release percentage of drug versus time. Fitting charts of release data was done using Origin software (Version 2021), and correlation coefficients (R^2) were obtained. Based on the comparison of correlation coefficients, the best model for release data was selected, and a Korsmeyer-Peppas model was employed to identify the drug release mechanisms [21]. According to n value, the drug release from a dosage form may occur through Fickian diffusion if $n < 0.43$, when $0.43 < n < 0.85$ it indicates a non-Fickian type release (a combination of both diffusion and erosion mechanisms). Also a greater value of n than 0.85 indicates the Case II transport (relaxation-controlled release). If $n > 1$, it indicates Super case II transport (swelling and polymer chain relaxation controlled release).

2.9. Animals

SPF-grade male Sprague-Dawley (SD) rats with a weight of 260 ± 20 g were supplied by Changsha Tianqin Biotechnology Co., Ltd. under certificate number SCXK (Xiang) 2019–0014. During a 12-h light/dark cycle, rats had free access to food and water at a constant room temperature of 20 ± 4 °C and humidity of 60 ± 10%. According to the Guide for the Care and Use of the Animal Management Rules of the Health Ministry of the People's Republic of China (documentation number 55, 2001, China), the animals were treated humanely, and the experimental protocol (No. 1801215) was approved by the Experimental Animal Ethics Committee of Guizhou Medical University.

2.10. Transient rat middle cerebral artery occlusion (MCAO) model

The Longa's suture technique [19,22,23] was used to simulate the transient occlusion of the middle cerebral artery (MCA) in rats. Before the operation, the rats were fasted for 12 h to reduce the mortality [24]. During the experiment, the anesthetized rats were immobilized on the rat fixture while lying in the supine position. A midline incision of the neck was made to isolate the common carotid artery (CCA), external carotid artery (ECA) and internal carotid artery (ICA). A tip-rounded monofilament nylon suture (d = 0.38 ± 0.02 mm, 45-mm length, 2838-A4, Beijing Cinontech Co. Ltd) was inserted into the ECA through the CCA into the ICA until there was complete blockage of the middle cerebral artery (MCA). Sham-operated animals were not subjected to I/R. To establish reperfusion, the nylon suture was removed 1 h after ischemia.

2.11. UPLC-ESI-MS/MS analysis for SCU in the plasma or the brain

A UPLC-ESI-MS/MS method was used to measure SCU in the brain [25] on a Waters Xevo TQ MS System (Waters, Milford, MA, USA). Data acquisition and analysis was performed by Mass Lynx V4.1 software (Milford, MA, USA). The LC separation was done on an Acquity I-Class UPLC system using an Acquity UPLC BEH C_{18} column (2.1 mm × 50 mm, 1.7 μm) protected by a Waters VanGuard BEH C_{18} column (2.1 mm × 5 mm, 1.7 μm) using a mobile phase containing of 0.2% formic acid water (A) and 0.2% formic acid in acetonitrile (B) at 40 °C. The gradient program was as follows: 0–0.5 min, 95%–95% A and 5%–5% B; 0.5–3 min, 95–5% A and 5–95% B; 3–3.5 min, 5–5% A and 95–95% B, 3.5–5 min, 5–95% A and 95–5% B. The peaks were obtained by injecting 1 μL of samples at a flow rate of 0.3 mL/min. SCU and puerarin (internal standard, IS) were detected in the positive ion mode following the optimized parameters: capillary voltage at 3 kV, collision energy at 20 V, cone voltage at 30 V for SCU and 40 V for puerarin. In the multiple reaction monitoring (MRM) mode, SCU and puerarin were quantified using the parent ion, *m/z* 463 for SCU and 417 for puerarin; and their daughter ion, *m/z* 287 for SCU and 267 for puerarin.

2.12. Effect of AMF intensity from LI-rTMS on the SCU levels in rat brain

The portable rTMS device with low intensity (LI-rTMS, NK-IA04, frequency 50 ± 1 Hz, Shijiazhuang Dukang Medical Instrument Co., Ltd) and its coils were shown in Fig. 1A and Fig. 1B. The intensity of

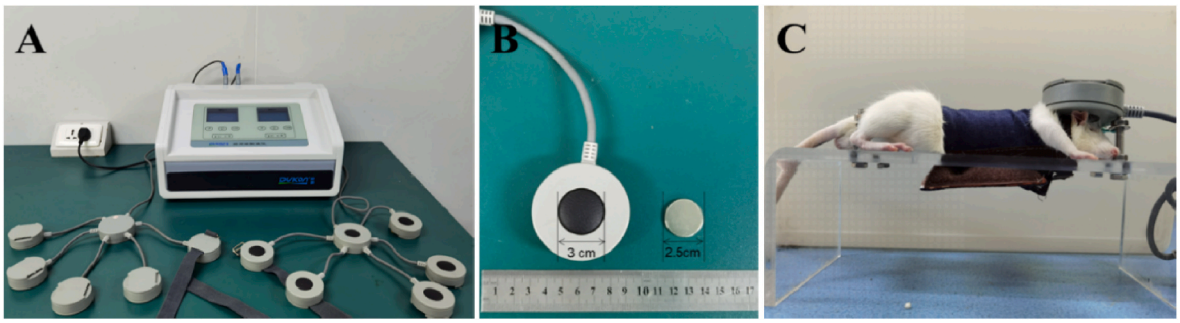

Fig. 1. The portable LI-rTMS device and the setup during the treatment. (A) The portable repetitive transcranial magnetic stimulator device. (B) The coil of portable rTMS and magnet. (C) The placement position of portable rTMS coil during the treatment.

alternating magnetic field (AMF) from LI-rTMS had three levels: Level I (3–5 mT), Level II (6–9 mT) and Level III (10–18 mT). The effect of different intensity produced by LI-rTMS on the SCU level in rat brain was investigated. The MCAO model rats were injected with SCU MNPs (SCU: 3.5 mg/kg, iron: 36.5 μg/kg) through the tail vein, then divided randomly into three groups (n = 5 in each group): Level I (3–5 mT), Level II (6–9 mT) and Level III (10–18 mT). The coil of LI-rTMS was immediately placed on the head of the rat as shown in Fig. 1C and fixed for 30 min. After AMF exposure of 30 min, the MCAO rat brain tissue was taken out at 40 min, weighed, and homogenized with 1:2 (w/v) normal saline. 100 μL of each tissue homogenate, 400 μL of methanol, 50 μL of 50 ng/mL puerarin solution, and 50 μL of 1% formic acid water were put into a 1.5-mL centrifuge tube, sonicated for 10 min and mixed evenly. The supernatant was dried under nitrogen at 37 °C after centrifugation at 12,000 rpm for 10 min at 4 °C. 1 μL of the resuspended sample in 200 μL of 50% methanol was injected for UPLC-ESI-MS/MS analysis.

2.13. Effect of AMF irradiation time from LI-rTMS on the SCU levels in rat brain

MCAO rats were administered with SCU MNPs (SCU: 3.5 mg/kg, iron: 36.5 μg/kg) through the tail vein, and randomized into three groups (n = 5 in each group): 10-min irradiation, 20-min irradiation, and 30-min irradiation. The coil of LI-rTMS was placed and fixed on the head of MCAO rats as mentioned in Fig. 1C with the output of Level II (6 mT ~ 9 mT) for different irradiation time (10 min, 20 min, 30 min). After administration, the rat brain tissue was quickly removed at 40 min, and the processing of brain tissue was the same as the procedure described in section 2.12. UPLC-ESI-MS/MS was used to measure the SCU level in the brain.

2.14. Effect of the iron addition in the formulation on the SCU levels in rat brain

The different addition of Fe_3O_4 NPs in the formulation resulted in the different attractive force by the magnetic field. Thus, the effect of different iron addition in the formulation on the SCU levels in rat brain was also investigated. Rats were randomly assigned into three groups after MCAO reperfusion (n = 5 in each group): 10 μg, 50 μg, and 90 μg of iron addition. Three different formulations of SCU MNPs (SCU: 3.5 mg/kg; iron: 7.3 μg/kg, 36.5 μg/kg, or 65.6 μg/kg) injected intravenously into the MCAO rat, respectively. After AMF irradiation for 30 min at Level II, the rat brain tissue was quickly removed at 40 min after administration, and the processing of brain tissue was the same as the procedure described in section 2.12. The SCU level in brain was measured by UPLC-ESI-MS/MS analysis.

2.15. Magnetic hyperthermia setup and protocol

In-vitro magnetic hyperthermia of 1.5 mL SCU MNPs (SCU: 1.5 mg/mL; iron: 0.03 mg/mL) or 1.5 mL saline was carried out under the AMF from LI-rTMS (NK-IA04, magnetic induction intensity: 6 mT ~ 9 mT, frequency: 50 ± 1 Hz, Shijiazhuang Dukang Medical Instrument Co., Ltd, China). Sample's temperature was recorded at 0 min, 30 min, 60 min and 120 min with a digital thermometer (WT-1, Elitech, Jiangsu, China) immersed in the central region of sample. The temperature change of 1.5 mL SCU MNPs without magnetic field or under a 0.2 T magnet were also measured as controls.

In-vivo thermal imaging and real-time temperature measurements of MCAO rats injected with SCU MNPs (SCU: 5 mg/kg; iron: 0.1 mg/kg) with/without the irradiation of magnetic field (0.2 T magnet or LI-rTMS) for 30 min were captured by an infrared thermal imaging camera (DW60-WS1 PLUS, Dali Technology, Zhejiang, China). The in-vivo thermal imaging and temperature measurement of MCAO rats injected with saline under the LI-rTMS for 30 min were also carried out as a control.

2.16. Pharmacokinetic study

Twelve SD rats were randomly divided into two groups of six each: SCU (SCU: 5 mg/kg) and SCU MNPs (SCU: 5 mg/kg; iron: 0.1 mg/kg), with the samples injected intravenously after MCAO reperfusion. The rat blood samples (0.15 ml) were collected at 0.083 h, 0.25 h, 0.5 h, 0.75 h, 1 h, 1.5 h, 2 h, 3 h, 4 h, 6 h, 8 h and 12 h after the administration into the centrifuge tubes containing EDTA-K2 (Jiangsu Kangjian Medical Apparatus Corporation, China) and centrifuged at 4000 rpm for 5 min at 4 °C. 50 μL supernatant, 25 μL 1% formic acid water solution, 25 μL of puerarin in methanol (50 ng/mL), and 200 μL methanol was added to the centrifuge tube and mixed for 2 min. After sonication and centrifugation, the supernatant was dried under nitrogen gas flow at 37 °C. The residue was resuspended in 200 μL 50% methanol and 1 μL of the supernatant was injected for UPLC-ESI-MS/MS analysis.

2.17. Distribution of SCU in MCAO rat brain

The MCAO rats treated with SCU or SCU MNPs were sacrificed by cervical dislocation at 2.5 h and 4 h. After removing and weighing the brain, it was homogenized quickly with 1:2 (w/v) normal saline and the processing of brain tissue was the same as the procedure described in section 2.12. The SCU level in brain was measured by UPLC-ESI-MS/MS analysis.

2.18. Pharmacodynamic treatment

MCAO rats were randomly assigned to seven groups: sham + saline, MCAO + saline, MCAO + saline + LI-rTMS, MCAO + free SCU group (SCU: 5 mg/kg/day), MCAO + SCU MNPs group (SCU: 5 mg/kg/day,

iron: 0.1 mg/kg/day), MCAO + SCU MNPs group (SCU: 5 mg/kg/day, iron: 0.1 mg/kg/day) + Magnet, MCAO + SCU MNPs group (SCU: 5 mg/kg/day, iron: 0.1 mg/kg/day) + LI-rTMS. As with the MCAO group, the sham group's rats received the same procedure, except that there was no blockage of the middle cerebral artery. MCAO rats and sham-operated rats were given 0.9% normal saline as controls. Prior to injection, free SCU was dissolved in PBS solution; the nano-suspensions containing SCU MNPs were prepared by ultrafiltration centrifugation using freshly prepared nanoparticles. One intravenous infusion of 1.5 ml/kg solution or nano-suspension was given each day for three days to rats. The intensity of AMF from LI-rTMS was set at Level II (6 mT ~ 9 mT) with a frequency of 50 ± 1 Hz and the irradiation time was 30 min. An NdFeB magnet (shape: cylindrical, diameter: 2.5 cm, thickness: 0.25 cm, 0.2 T, Ningbo lianghao Magnetic Industry Co., Ltd) was placed on the head of MCAO rats as the same as LI-rTMS shown in Fig. 1C for 30min. After administration, both the static magnetic field (SMF) of the magnet and the alternating magnetic field (AMF) of LI-rTMS were immediately applied once a day for 3 days.

2.19. Neurological evaluation

MCAO rats were evaluated for neurological function 24 h after reperfusion with the Zea-Longa score method [22–24]. The neurological behaviours were assessed on a 5-point scale: 0- no neurological deficits (normal); 1- lack of ability to extend forepaw completely (mild); 2- having difficulty keeping balance while walking (moderate); 3- falling (severe); 4- inability to walk spontaneously and loss of consciousness (very severe). Following the successful establishment of the rat MCAO model, rats with neurological deficit score 1–3 can be used for further experiments. After the third dose, the rat neurological behaviour was evaluated again by the blinded experimenter according to the above score method.

2.20. Changes of bodyweight

Before surgery and three days after treatment, all rats were weighed. The changes in body weight are expressed as a percentage compared to its pre-ischemia weight for each animal following ischemia.

2.21. TTC assessment of cerebral infarct area

Infarcts of sham-operated rats and MCAO rats after the treatments with normal saline, SCU, SCU MNPs or different combinations with magnetic fields were evaluated by 2,3,5-triphenyltetrazolium chloride (TTC) staining [19]. After the third dose, the rats were sacrificed and their brains were removed. The frozen brain tissue was cut into five 2 mm thick coronal sections. The area of cerebral infarction was quantified with TTC (Sigma Aldrich, USA) staining. Infarcted areas appeared white, while normal areas appeared red. Image Pro Plus software was used to measure cerebral infarction areas in each section, and the following formula was used to calculate cerebral infarction areas:

$$\text{brain infarct area} = \frac{\textit{white brain area}}{\textit{the whole brain area}} \times 100\% \quad (10)$$

2.22. Hematoxylin and Eosin (H&E) staining

Each group of brain samples was collected following the procedure [19] described in section 2.21. Staining the brain tissues with hematoxylin and eosin followed standard protocols. Each group of rats was examined under an optical microscope for changes in the morphology of the hippocampus and cortex due to cerebral ischemia.

2.23. TUNEL assay

Each group of brain samples was collected following the procedure described in section 2.21. According to the manufacturer's instructions, the brain tissues were stained with the FITC-labelled TUNEL kit (Servicebio Technology Co., Ltd., Wuhan, China) and counterstained with DAPI solution. The slices were observed by a Nikon Eclipse C1 fluorescence microscope. The stained slides were scanned with a panoramic slide scanner (PANNORAMIC DESK/MIDI/250/1000, 3DHISTECH Ltd., Hungary). The normal cells were stained with blue by DAPI (UV excitation wavelength: 330–380 nm; emission wavelength: 420 nm) and the apoptotic cells were stained with green by FITC (excitation wavelength: 465–495 nm; emission wavelength: 515–555 nm). An Indica Labs-HighPlex FL v3.1.0 module in Halo v3.0.311.314 software (USA) was used to quantify the number of positive apoptosis cells and total cells in each slice. The positive apoptosis rate (%) was calculated by the following formula:

$$\text{Positive apoptosis rate} = \frac{\textit{number of positive cells}}{\textit{number of total cells}} \times 100\% \quad (11)$$

2.24. Determination of SOD, MDA, NO, TNF-α and IL-6 levels in the serum

Six rats per group were given continuous administration for 3 days, then blood was collected from their femoral arteries and centrifuged at 3500 rpm for 10 min after standing at room temperature for 1–2 h. The supernatant was taken, divided and stored in refrigerator at −20 °C. The levels of SOD, MDA, and NO levels in the serum were determined by spectrophotometry according to the instructions of SOD, MDA and NO kits (Nanjing Jiancheng Bioengineering Institute, Nanjing, China). Serum TNF-α and IL-6 contents were detected by ELISA (Shanghai Zhuocai Biotechnology Co., Ltd, Shanghai, China).

2.25. Statistical analysis

In this study, WinNonLin 8.2 software was used to obtain the pharmacokinetic parameters and SPSS 19.0 to analyse all the experimental data. Independent-samples *t*-test was used for the pharmacokinetic results. Kruskal-Wallis non-parametric test (K–W test) was used in the statistical analysis of neurological deficit score. One-way analysis of variance (ANOVA) was used to analyse the cerebral infarction area, change in bodyweight, neuronal apoptosis and in vivo magnetic hyperthermia. Data were expressed as mean ± SD of at least three independent experiments. Statistical significance was defined as a P value of less than 0.05.

3. Results

3.1. Preparation and characterisation of SCU MNPs

SCU MNPs were prepared by the nanoprecipitation method as illustrated in Fig. 2A. The obtained SCU MNPs were brown yellow and can be attracted and recruited by the magnet (Fig. 2B). Under the observation of transmission electron microscope (TEM), SCU MNPs were spherical with diameter in the range of 75–180 nm (Fig. 2C) while the hydrodynamic diameter was around 190 nm shown in Fig. 2D. In the UV–Vis spectra (Fig. 2E), SCU had a characteristic double peak at 280 nm and 335 nm while MNPs had no peak in this area. Through the encapsulation of MNPs, the unique double peak shape appeared in the SCU MNPs, which implied that SCU was successfully loaded in the MNPs. In the FTIR spectra (Fig. 2F), SCU MNPs had the similar fingerprint spectra with MNPs, which also verified the successful embedding of MNPs in the SCU MNPs.

3.2. Effect of the AMF conditions and iron addition in the formulation on the SCU levels in MCAO rat brain

The magnetic force for the drug targeting was decided by the

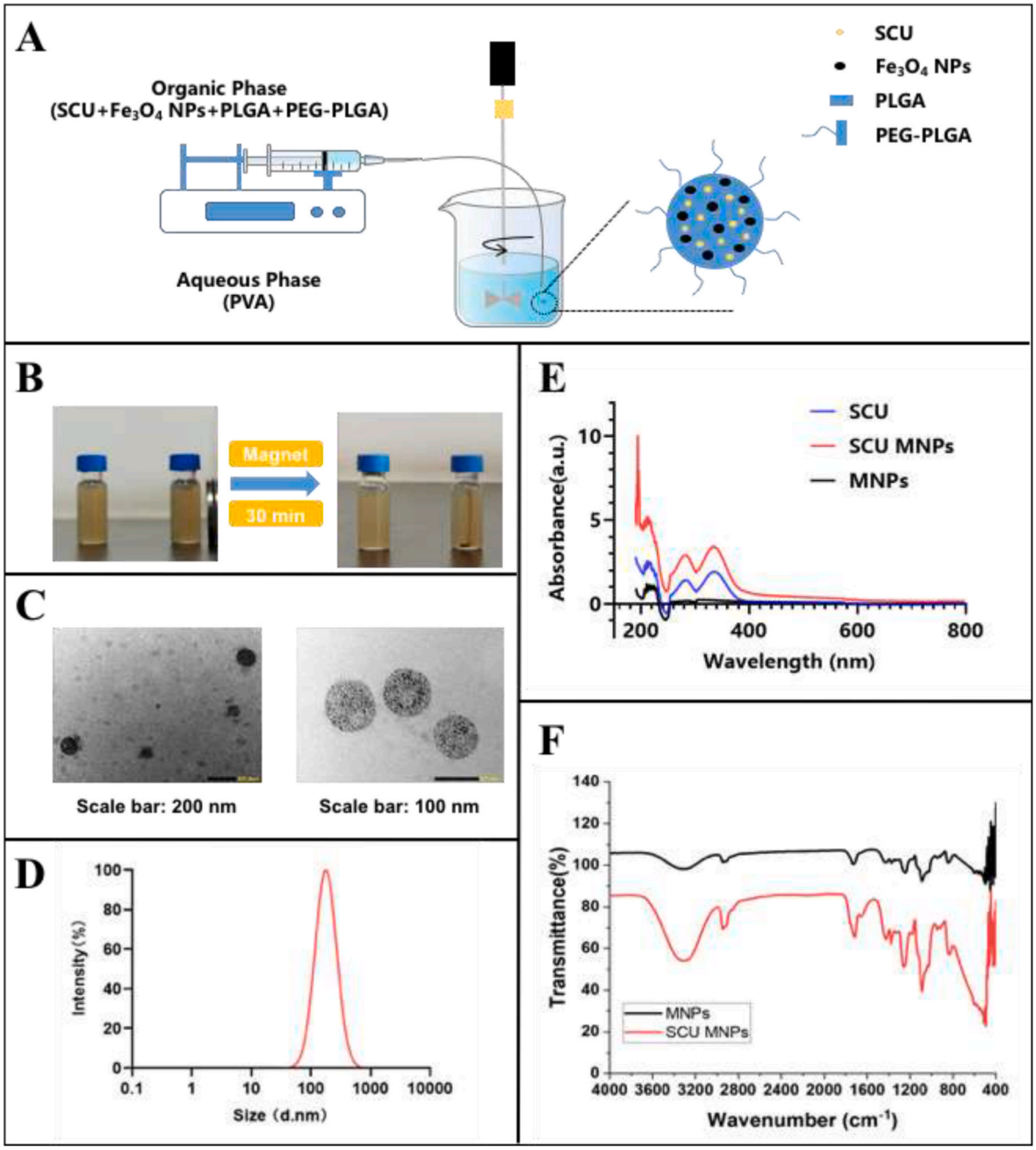

Fig. 2. Scheme of SCU MNPs preparation and physicochemical characterisation of SCU MNPs. (A) Scheme of SCU MNPs preparation by nanoprecipitation. (B) Photographs showing SCU MNPs suspension in water and recruitment of SCU MNPs towards a 0.2 T magnet. (C) TEM images of SCU MNPs. (D) The hydrodynamic diameter measured by a Nanobrook 90Plus PALS particle size analyser (Brookhaven Instruments, New York, USA). (E) UV–Vis spectra of SCU, MNPs and SCU MNPs. (F) FTIR spectra of MNPs and SCU MNPs.

conditions of magnetic field and iron addition in the formulation. Thus, the effect of AMF intensity, irradiation time and iron addition in the formulation on the SCU level in MCAO rat brain were investigated by UPLC-ESI-MS/MS analysis as shown in Fig. 3. Fig. 3A showed the typical chromatograms of SCU (b,c) and puerarin (e,f) as the internal standard in the blank serum and sample serum in the MRM mode. It is evident that the SCU level (3–4 μg/g) in MCAO rat brain increased as a function of the AMF irradiation time (10–30 min) from LI-rTMS (Fig. 3B). The effect of AMF intensity on the SCU level in the brain was complex. The AMF may drive one particle toward its target and drive another particle away from it [26]. As shown in Fig. 3C, the AMF intensity of Level II (6–9 mT) can bring more SCU (7.39 μg/g) in the brain rather than the higher AMF intensity of Level III (10–18 mT, SCU: 5.91 μg/g) or lower AMF intensity of Level I (3–5 mT, SCU 6.36 μg/g) ($P < 0.05$). The iron addition in the formulation of SCU MNPs was the most important factor on the drug targeting driven by the nanoparticles. Fig. 3D showed the highest SCU level (6.49 μg/g) in rat brain at the iron addition of 90 μg in the formulation. Unfortunately, the iron addition had a minimum effect on the SCU in the brain (<3.87 μg/g) if the iron addition was less than 50 μg.

3.3. Stability of SCU MNPs in one month

In the interest of making SCU MNPs storage as convenient as possible, the stability of the optimal SCU MNPs was evaluated by the change of hydrodynamic diameter and SCU DL at room temperature or

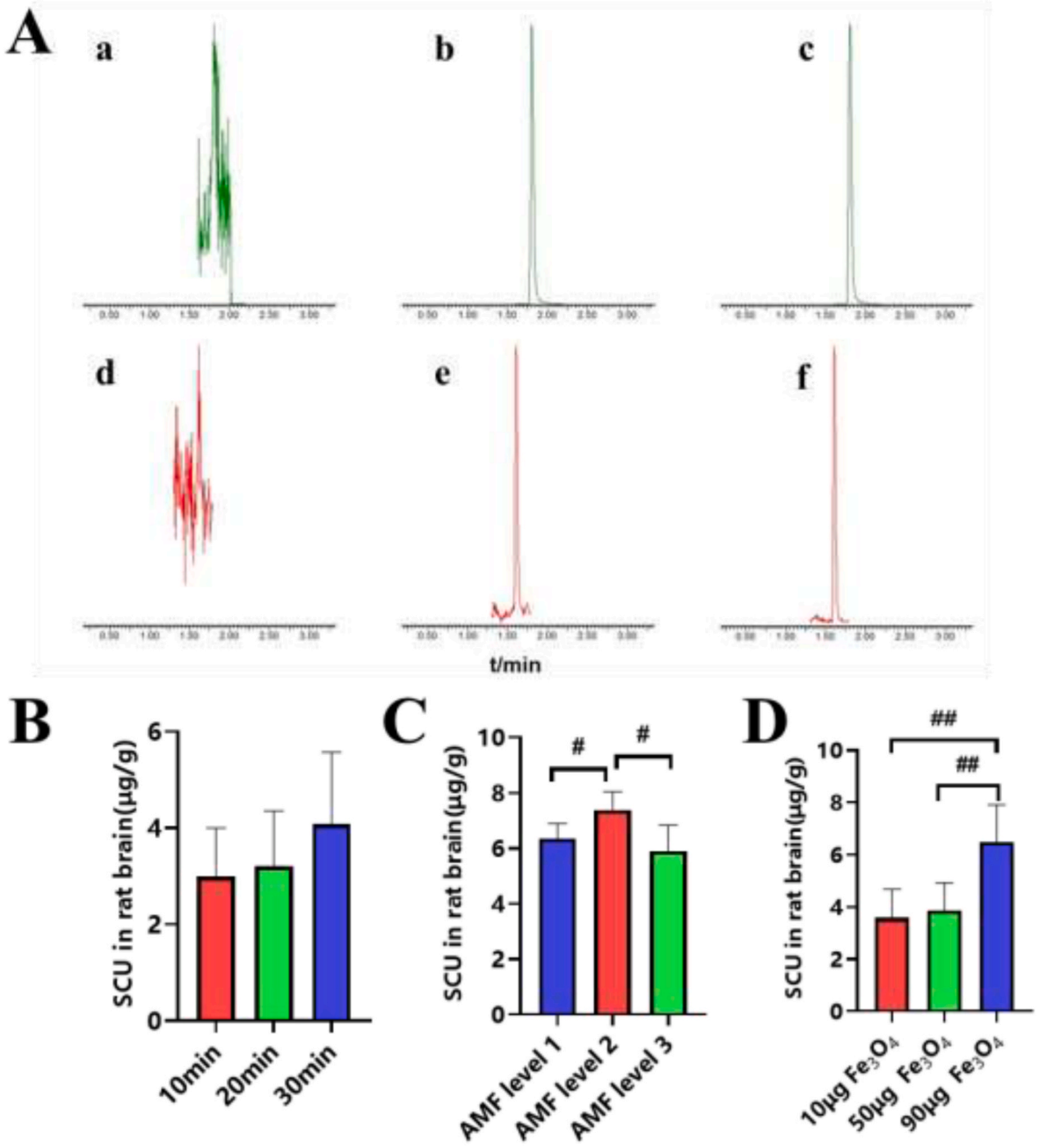

Fig. 3. The effect of portable LI-rTMS condition and iron addition in the formulation on the SCU level in the MCAO rat brain.(A) Base peak chromatograms of SCU (a, b,c) and puerarin (d,e,f) as the internal standard in the MRM mode. (a) and (d) blank serum; (b) and (e) standard reference in the blank serum; (c) and (f) sample serum. (B) The effect of the irradiation time of LI-rTMS on the SCU in MCAO rat brain. (C) The effect of the magnetic field intensity of LI-rTMS on the SCU in MCAO rat brain. (D) The effect of the addition of iron content in the formulation on the SCU in MCAO rat brain. Data shown as mean ± standard deviation (SD) (n = 5). Statistical analysis was performed using one-way analysis of variance (ANOVA). $^{\#}P < 0.05$, $^{\#\#}P < 0.01$.

at 4 °C. As illustrated in Fig. 4, the size of SCU MNPs were little changed at room temperature (<10%) or at 4 °C (<6%) for 30 days while the DL of SCU MNPs decreased 21.85% at room temperature and 13.42% at 4 °C in one month. It is safely concluded that SCU MNPs were more stable at 4 °C. For the storage period, 90% SCU was required in the formulation. The SCU remaining in the formulation at room temperature and at 4 °C were 93% at 14 and 7 days, respectively. Thus, SCU MNPs can be stored at 4 °C for 14 days and at room temperature for 7 days.

3.4. Profile of drug release by SCU MNPs in vitro

Fig. 5 illustrated the release profile of SCU MNPs in PBS containing 2 mg/mL EDTA-2Na at 37 °C. *In vitro*, SCU MNPs released rapidly during the first 4 h, followed by a prolonged release over the next 20 h [27,28]. SCU absorbed on the nanoparticle surface mainly accounted for the fast initial release. Moreover, encapsulated SCU may diffuse from the inner part of nanoparticles explaining slower release. Various kinetic models were used to assess the dissolution profile of SCU from formulation, including zero order, first order, Higuchi, Hixson-Crowell, and Korsmeyer-Peppas. The mathematical models, equations and correlation coefficients were presented in Table 1. For all formulations, Hixson-Crowell model provided the best in vitro release pattern explanation ($R^2 = 0.9791$) followed by first order ($R^2 = 0.9704$). With the progressive dissolution of PLGA polymers, the Hixson-Crowell model

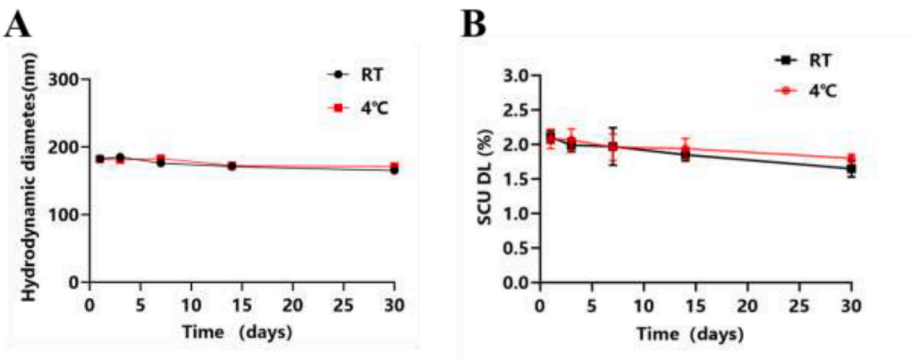

Fig. 4. The change of hydrodynamic diameter (A) and SCU DL (B) of SCU MNPs at room temperature and 4 °C. Data are expressed as mean ± standard deviation (SD) (n = 3). Error bars smaller than the symbols are not visible.

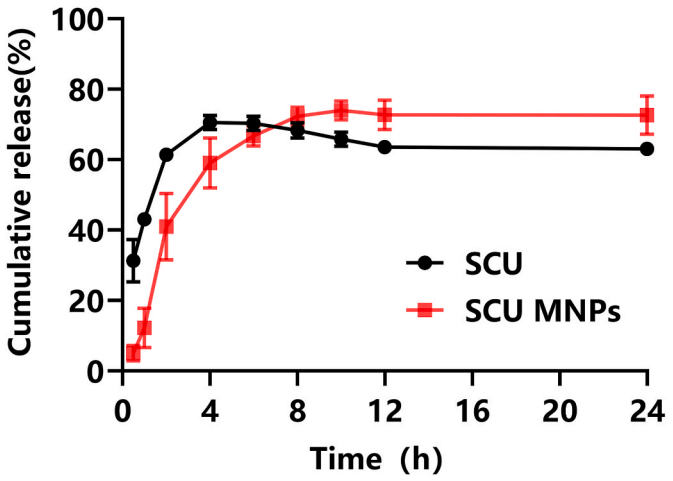

Fig. 5. *In-vitro* drug release from SCU and SCU MNPs in PBS (pH 7.4) containing 2 mg/mL EDTA-2Na at 37 °C. 1.5 mL of SCU or SCU MNPs put in a dialysis bag were soaked in 30 mL PBS solution with 2 mg/mL EDTA-2Na at 37 °C. Samples were collected from the external medium at time intervals of 0.5 h, 1 h, 2 h, 4 h, 6 h, 8 h, 10 h, 12 h, 24 h, and the cumulative SCU release was assessed using a HPLC method at a wavelength of 335 nm. The results are expressed as mean ± standard deviation (SD) (n = 3). The error bars are not visible if they are smaller than the symbols.

Table 1
Release kinetic parameters for drug release from SCU MNPs fitted to various pharmacokinetics models.

Model	Equation	R^2
Zero-order	$M_t/M_\infty = 2.5270t+33.8890$	0.4694
First-order	$M_t/M_\infty = 75.5743(1-e^{-0.3357t})$	0.9704
Higuchi	$M_t/M_\infty = 17.2200t^{1/2}+10.8920$	0.7061
Hixson-Crowell	$M_t/M_\infty = 0.0430t^{3}-1.7902t^{2}+21.2871t-3.1516$	0.9791
Korsmeyer-Peppas	$M_t/M_\infty = 111422.8229t^{1.8537}-111400.3353$	0.9064

showed a change in surface area and diameter of the nanoparticles over time. First order model described the concentration dependent release of SCU from nanoparticles. A Korsmeyer-Peppas equation was also fitted to the data to illustrate further the drug release mechanism. According to Table 1, the formulation showed a strong correlation ($R^2 = 0.9064$) with the mathematical model and the calculated value of release exponent (n) was 1.8537. PLGA nanoparticles may release SCU via Super case II transport (swelling and polymer chain relaxation controlled release), which was consistent with the reported release mechanism of PLGA based nanoparticles [29,30].

3.5. Magnetic hyperthermia of SCU MNPs combination with magnetic field

Magnetic hyperthermia is based on the heat production by MNPs under alternating magnetic field (AMF) exposure. While most hyperthermia techniques currently in development are targeted towards cancer treatment [31–34], some side effects are also reported such as heat pain [35], evenly heat shock [36]. Regarding to the magnetic nanoparticles in the central nervous system, AMF can increase the blood brain barrier (BBB) permeability by magnetic heat [26]. Thus, *in-vitro* and *in-vivo* magnetic hyperthermia of SCU MNPs induced by magnetic field was investigated. Fig. 6A represented the temperature change (ΔT) of SCU MNPs (SCU: 1.5 mg/mL; iron: 0.03 mg/mL) with the exposure of 0.2 T magnet or LI-rTMS (6–9 mT, 50 ± 1 Hz). The temperature changes of SCU MNPs or LI-rTMS alone over 2 h were also carried out as controls. As indicated in Fig. 6A, ΔT of SCU MNPs or LI-rTMS alone over 2 h was minimal (<0.5 °C). With the exposure of SMF (0.2 T magnet), the temperature of SCU MNPs slightly increased (0.53 ± 0.40 °C) at 0.5 h then gradually decreased (−0.47 ± 0.45 °C) at 2 h. As predicted, the temperature change of SCU MNPs with the exposure of AMF from LI-rTMS increased, and reached the top at 2 h (1.90 ± 0.30 °C), which confirmed the hyperthermia induced by SCU MNPs combination with AMF.

In our further *in-vivo* experiment, magnetic hyperthermia of MCAO rats after administration of SCU MNPs or saline following the magnetic field exposure of 30 min was observed by an infrared thermal imaging camera (DW60-WS1 PLUS, Dali Technology, Zhejiang, China) as shown in Fig. 6B. The real-time temperature measurements of MCAO rat head after the different treatments were also recorded by the infrared thermal imaging camera as shown in Fig. 6C. Consistent with the *in-vitro* results, the heads of MCAO rat treated with SCU MNPs or LI-rTMS alone exhibited negligible colour change as well as an insignificant temperature elevation. A trivial decrease of temperature was found in the group of SCU MNPs under SMF exposure of 30 min. After the exposure of AMF for 30 min, the head temperature of MCAO rats administrated by SCU-MNPs increased significantly ($P < 0.05$), further verifying the hyperthermia of SCU MNPs combination with AMF.

3.6. SCU MNPs increase SCU level in MCAO rats' blood and brain

MCAO rats were given intravenously 5 mg/kg of SCU or SCU MNPs for three consecutive days to mimic the dose used in therapy [37,38]. Blood was collected at various points after the last dose. SCU was extracted from blood and quantified by UPLC-ESI-MS/MS method. The plasma profile and pharmacokinetics parameters of SCU MNPs and free SCU in the MCAO rat model were depicted in Fig. 7A and Table 2. The blood clearance of SCU MNPs was comparable to free SCU in the first 0.083h (5 min) post injection. Similar to our *in-vitro* drug release observations, the reason was likely free SCU absorbed onto the surface of

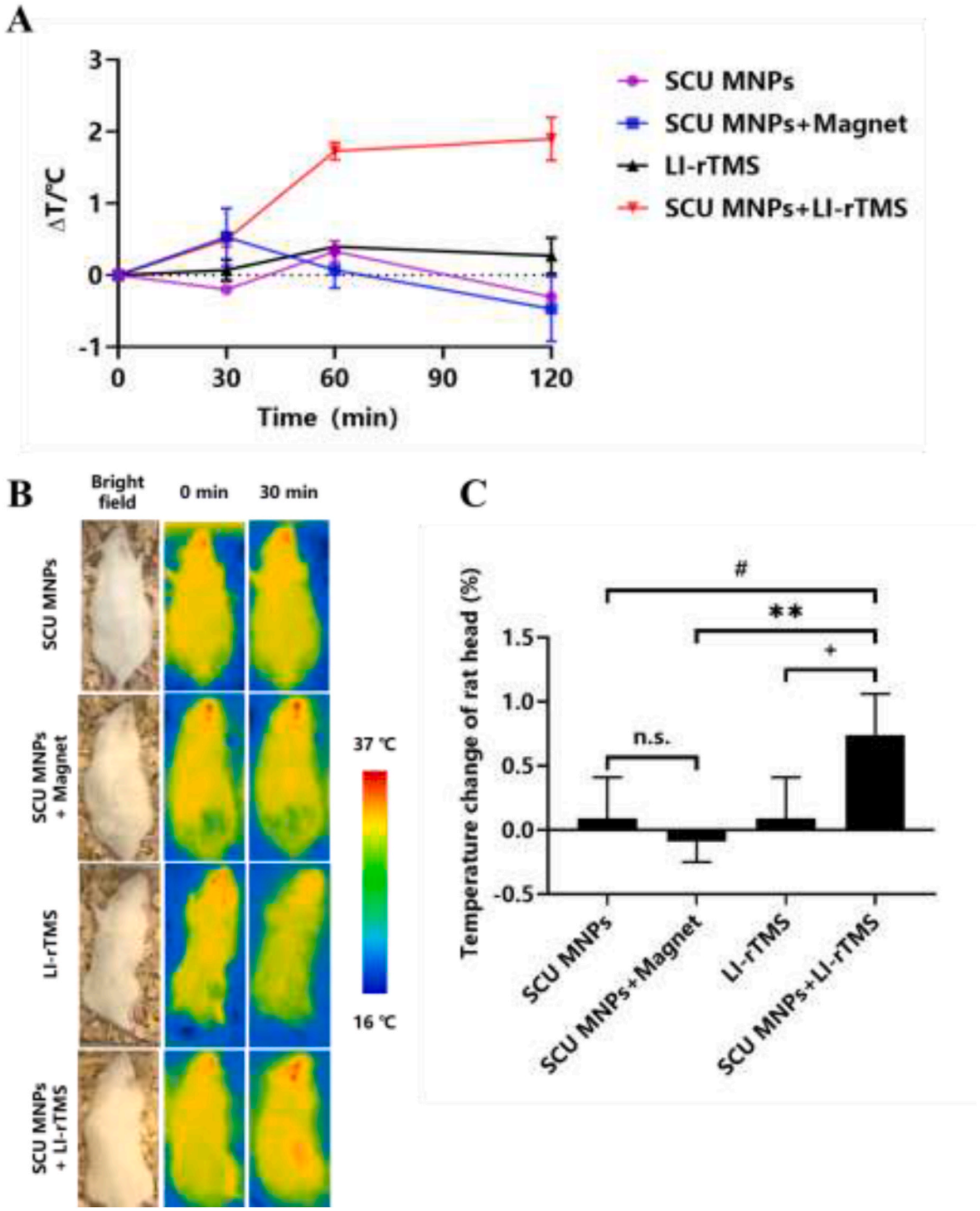

Fig. 6. Magnetic hyperthermia of SCU MNPs with the exposure of magnetic field. (A) The temperature change of saline or SCU MNPs under the exposure of magnet or the LI-rTMS device for 2h. (B) Thermal images of MCAO rats injected with saline or SCU MNPs with the exposure of magnet or LI-rTMS for 30 min. (C) The temperature changes of MCAO rat head based on the thermal imaging. Data are presented as average ± SD (n = 3). One-way analysis of variance (ANOVA) was employed for the statistical analysis. $^{\#}$ denotes comparison with SCU MNPs group ($^{\#}P < 0.05$). * denotes comparison with SCU MNPs + Magnet group ($^{*}P < 0.05$, $^{**}P < 0.01$). + denotes comparison with LI-rTMS group ($^{+}P < 0.05$). N.s. means not statistically significant.

SCU MNPs. However, the AUC of SCU in the SCU MNPs had a 2-fold increase ($P < 0.01$) from 0.25 h (15 min) to 12 h (47.14 ± 12.82 vs 23.83 ± 4.37 h × μg/mL) revealed in Table 2, indicating that SCU MNPs provided a significantly higher SCU concentration in the systemic circulation (mean plasma concentration: 3.93 ± 1.07 μg/mL vs 1.99 ± 0.36 μg/mL) and for an extended period of time (mean retention time MRT: 1.59 ± 0.29 vs 0.37 ± 0.04 h). The results are consistent with other reports showing extended drug circulation after NPs encapsulation [39].

Fig. 7B showed the change of SCU level in MCAO rat brain affected by the formulation and magnetic field. SCU was less in the brain at 4 h compared with that at 2.5 h while SCU MNPs had more SCU in the brain at 4 h, implying that SCU improved the stability of SCU in the body fluid. Compared with SCU MNPs without the exposure to magnetic field, SCU

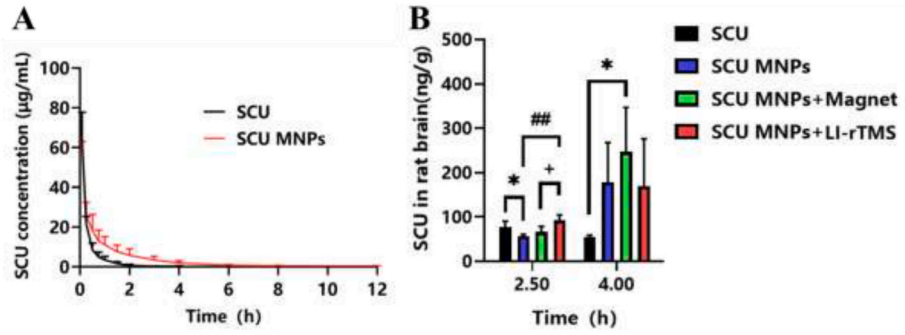

Fig. 7. Plasma profile (A) and brain level (B) of SCU MNPs and free SCU administered intravenously in MCAO rats. (A) SCU (5 mg/kg) and SCU MNPs (SCU: 5 mg/kg; iron: 0.1 mg/kg) were given intravenously (via tail vein) every day for 3 days following the MCAO operation. Detection of SCU in rat plasma was done using the UPLC-ESI-MS/MS method, and the samples were collected at 0.083, 0.25, 0.5, 0.75, 1, 1.5, 2, 3, 4, 6, 8 and 12 h after the last dose. Data are shown as mean ± SD (n = 6). (B) After the last dose, SCU brain levels in rats were collected at 2.5 h and 4 h after treatment as described in (A). Data are presented as average ± SD (n = 3). One-way analysis of variance (ANOVA) was employed for the statistical analysis. * denotes comparison with free SCU group ($^{*}P < 0.05$). $^{\#}$ denotes comparison with SCU MNPs group ($^{\#\#}P < 0.01$). + denotes comparison with SCU MNPs + Magnet group ($^{+}P < 0.05$).

Table 2
Pharmacokinetic parameters obtained after intravenously administration of free SCU and SCU MNPs in MCAO rats at a dose of 5 mg/kg SCU once a day for 3 days. Data are shown as mean ± SD (n = 6). Statistical analysis was performed using the independent-samples T test by SPSS software 19.0. * denotes comparison between SCU and SCU MNPs ($^{*}P < 0.05$, $^{**}P < 0.01$, $^{***}P < 0.001$).

	Unit	SCU	SCU MNP
$t_{1/2}$	h	0.59 ± 0.12	1.84 ± 0.19***
AUC_{0-t}	μg*h/mL	23.83 ± 4.37	47.14 ± 12.82**
$AUC_{0-\infty}$	μg*h/mL	24.12 ± 4.46	48.09 ± 12.99**
Cl_z	L/h/kg	213.04 ± 37.95	111.37 ± 33.25**
V_z	L/Kg	182.85 ± 52.38	297.12 ± 99.39*
MRT	h	0.37 ± 0.04	1.59 ± 0.29***
$MRT_{0-\infty}$	h	0.42 ± 0.04	1.85 ± 0.35***

$t_{1/2}$, terminal elimination half-life; AUC_{0-t}, area under plasma concentration versus time curve from zero to last sampling time; $AUC_{0-\infty}$, area under plasma concentration versus time curve from zero to infinity; Cl_z, total body clearance; V_z, apparent volume of distribution; MRT, mean retention time from zero to last sampling time; $MRT_{0-\infty}$, mean retention time from zero to infinity.

MNPs can carry more SCU into the brain (92.79 ± 12.20 vs 56.33 ± 4.09 ng/g) at 2.5 h under the guidance of the AMF exposure from LI-rTMS ($P < 0.01$). More importantly, the AMF exposure (LI-rTMS) produced a significant increase of SCU driven by SCU MNPs than SMF (Magnet) (92.79 ± 12.20 vs 66.66 ± 12.44 ng/g) at 2.5 h ($P < 0.05$), although these significances disappeared at 4 h due to the withdrawal of the magnetic force.

3.7. The intravenous administration of SCU MNPs with AMF exposure can improve rat behavioural symptoms and recover cerebral ischemia

Massive ischemia damaged the cerebral cortex on the ipsilateral side as a result of MCAO. 2,3,5-Triphenyltetrazolium chloride (TTC) staining was used to evaluate the infarct area after MCAO and following SCU, SCU MNPs, or SCU MNPs with different levels of magnetic field exposure (Fig. 8A), and Image J software was used to measure infarct areas in each section shown in Fig. 8B. Compared with the model groups, sham-operated rats had the same procedure, but they were not sutured at the middle cerebral artery. Thus, no obvious and massive white ischemia infarct areas were present in sham-operated rats. In contrast, MCAO rats had white infarctions in ipsilateral hemispheric brain slices. Compared with the MCAO model group, the area of cerebral infarction in the LI-rTMS group was not significantly reduced (32.51 ± 4.43% vs 35.76 ± 3.51%), suggesting the low intensity of alternating magnetic field from LI-rTMS (6–9 mT, 50 ± 1 Hz) could not have the therapeutic effect on the cerebral infarction. Following treatment with free SCU or SCU MNPs alone, the infarct volume was progressively reduced (26.83 ± 3.34% and 22.07 ± 3.63%, respectively), which indicated that SCU can improve the cerebral ischemia and the SCU MNPs were better. The reason behind this improvement of SCU MNPs was perhaps the increase of nanoparticles for SCU stability and concentration in the plasma and brain seen in the in-vitro release experiment and in vivo pharmacokinetic studies. Compared with free SCU MNPs, with the exposure of 0.2 T magnet, there was no significance in attenuating the ischemia area (21.57 ± 3.29%) while with LI-rTMS, the infarct volume was the least (16.48 ± 4.76%). It is implied that LI-rTMS can guide more SCU MNPs into the brain than magnet due to the deeper penetration of AMF. Behavioural study showed a significant decline in neurological scores in MCAO rats by Longa score method especially for the SCU MNPs group with the exposure of LI-rTMS ($P < 0.01$) shown in Fig. 8C. Three days after MCAO, rats only with the exposure of LI-rTMS showed a clear neurological deficit with a neurological score of 3.00 ± 0.63. But the neurological score of SCU and SCU MNPs were lower than the MCAO model group (3.33 ± 0.52) with a value of 2.00 ± 0.63 and 1.67 ± 0.52, respectively, which indicated that SCU can protect the cerebral ischemia infarct, interestingly SCU MNPs were better than SCU. In combination with magnetic field, LI-rTMS can further enhance the therapeutic efficacy of SCU MNPs than magnet (1.33 ± 0.52 vs 1.67 ± 0.52). As shown in Fig. 8D, the body weight of the ischemic rats continued to decline until postoperative day 3. In the MCAO and LI-rTMS groups, the body weight of MCAO rats decreased approximately 25%, while in the SCU and SCU MNPs treated groups, the body weight of MCAO rats decreased 17.52 ± 1.89% and 20.40 ± 3.09%, respectively. After administration of SCU MNPs combined with the magnetic field, the decrease of rat body weight in the magnet group was comparable to free SCU MNPs (19.72 ± 5.06%) while the decrease of rat body weight in the LI-rTMS group was the least (10.78 ± 4.34%), consistently confirming the higher efficacy of SCU MNPs with the exposure of LI-rTMS in rescuing cerebral ischemia in rats.

3.8. SCU MNPs with the exposure of LI-rTMS can reverse histopathological changes in hippocampus and cortex cells of brain tissues

Hematoxylin and eosin (H&E) staining revealed the cerebral ischemia/reperfusion injury patterns in hippocampus and cortex areas shown in Fig. 9. In the infarcted cerebral areas of the MCAO rat model, the H&E stained brain tissue was lighter to suggest liquefactive necrosis [40]. In the hippocampus region, a loosely arranged structure (blue arrow) and hemorrhage in the corpus collosum (grey arrow) occurred in the saline-treated MCAO model group while no abnormalities were observed in the sham-operated groups. Hippocampus of the SCU MNPs group also displayed loose arrangement and hemorrhage in the corpus collosum. In the SCU and SCU MNPs combined with LI-rTMS groups, an arrangement of single neurons shrank similar to the sham-operated group, confirming that SCU was able to reverse the damage induced by MCAO. In the cortex area, sham-operated groups had normal and uniform tissue structure without obvious degeneration, inflammation and necrosis of neurons. The nuclear pyknosis (red arrow), neuronal cell

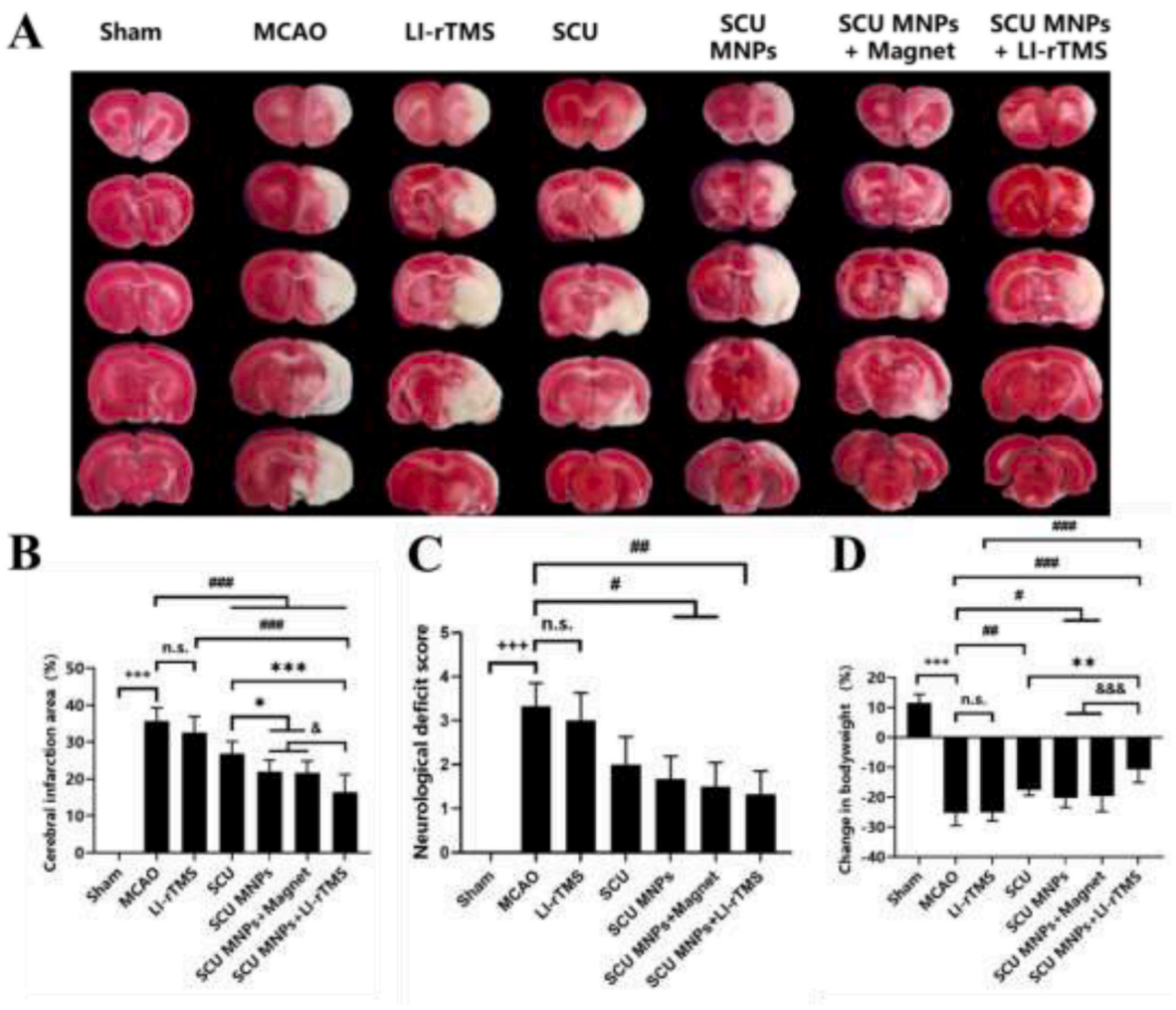

Fig. 8. An intravenous injection of SCU MNPs under the magnetic field improved the rats' behaviour and rescued cerebral ischemia in rats. Examinations of the infarct size, neurological deficits, and bodyweight changes in rats at 3 days were carried out following different treatments. (A) Representative images of TTC-stained brain slices (all 5 slices in one rat brain, n = 1); (B) Analysis of cerebral infarction area; (C) Neurological deficit scores in rats; (D) postoperative bodyweight change in rats. Data are presented as average ± SD (n = 6). One-way analysis of variance (ANOVA) was employed for the statistical analysis. + denotes comparison with sham group ($^{+++}P < 0.001$). # denotes comparison with MCAO group or LI-rTMS ($^{\#}P < 0.05$, $^{\#\#}P < 0.01$, $^{\#\#\#}P < 0.001$). * denotes comparison with SCU group ($^{*}P < 0.05$, $^{**}P < 0.01$, $^{***}P < 0.001$). & denotes comparison with SCU MNPs group or SCU MNPs + Magnet group ($^{\&}P < 0.05$, $^{\&\&\&}P < 0.001$). N.s. means not statistically significant.

necrosis and nuclear dissolution (yellow arrow) were seen in the MCAO, LI-rTMS, SCU, SCU MNPs and SCU MNPs + Magnet groups. The increase of the number of neurons and relatively regular morphology in the SCU MNPs combined with LI-rTMS group were observed, which confirmed that SCU MNPs combined with LI-rTMS have a better effect on the treatment of MCAO injury.

3.9. SCU MNPs combined with LI-rTMS can alleviate cerebral ischemia-induced neuronal apoptosis

Apoptosis in neuronal regions of brain slices was confirmed by TUNEL staining (Fig. 10A), and a quantitative analysis of apoptosis in the ischemic cortex from each slide of three rats per group was shown in Fig. 10B. The sham-operated group did not exhibit signs of apoptosis in TUNEL-stained brain sections, suggesting that very little damage occurred to the brain during the sham operation. As expected, more TUNEL-positive cells were observed in the ischemic hemisphere of saline with/without LI-rTMS treated diseased rats (6.11 ± 1.12% and 7.63 ± 1.58%, respectively), confirming the extensive apoptotic response to ischemia-reperfusion injury. Interestingly, the number of TUNEL-positive cells significantly reduced in MCAO rats treated with SCU (3.79 ± 1.63%) or SCU MNPs (3.40 ± 0.92%). In agreement with earlier results (Figs. 8 and 9), SCU MNPs in combination with magnetic field significantly reduced the percentage of apoptotic cells in the ischemic cortex. In contrast to the SMF from magnet (2.67 ± 1.93), the decrease of TUNEL-positive cells was greater when combined with AMF from LI-rTMS (1.30 ± 0.69), which further confirms that SCU MNPs combined with LI-rTMS provided a better protective effect than free SCU or SCU MNPs at an equivalent dose against cerebral I/R injury.

3.10. SCU MNPs combined with LI-rTMS can reduce the oxidative stress and inflammatory levels after cerebral I/R injury

To investigate the possible synergistic mechanism of SCU MNPs combined with LI-rTMS, the levels of SOD, MDA, NO, TNF-α and IL-6 levels in the serum of MCAO rats were determined by commercial kits. There was a significant difference in the SOD activity (Fig. 11A), as well as a decrease in the MDA (Fig. 11B) and NO levels (Fig. 11C) for SCU ($P < 0.01$), SCU MNPs ($P < 0.05$), LI-rTMS ($P < 0.05$) and SCU MNPs + LI-rTMS ($P < 0.001$) when compared with MCAO group, which investigated the anti-oxidant activity of SCU and LI-rTMS. Compared to SCU, SCU MNPs and LI-rTMS alone, SCU MNPs coupled to LI-rTMS had a

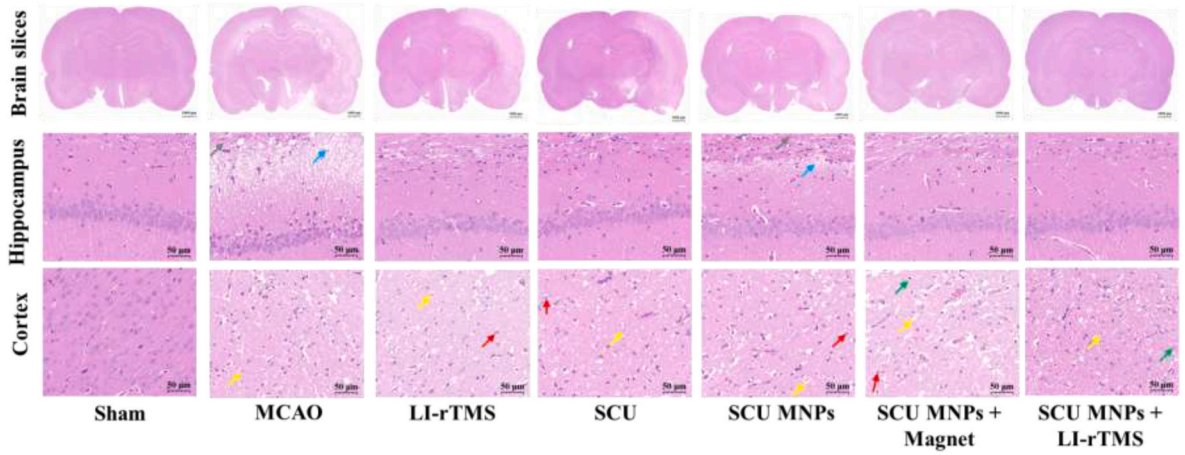

Fig. 9. SCU MNPs under the magnetic field guidance reversed histopathological changes in brain tissues of MCAO rats. Typical images of H&E-stained brain slices (scale bar: 1000 μm), hippocampus and cortex (scale bar: 50 μm) of sham-operated rats, and MCAO rat models treated with saline ± LI-rTMS, free SCU, SCU MNPs, SCU MNPs + Magnet, and SCU MNPs + LI-rTMS. Blue arrow represented loosely arranged structure; grey arrow represented the hemorrhage in corpus callosum; yellow arrows represented neuronal cell necrosis and nuclear dissolution; red arrow represented the nuclear pyknosis with irregular shape; green arrow represented the glial cells. (For interpretation of the references to colour in this figure legend, the reader is referred to the Web version of this article.)

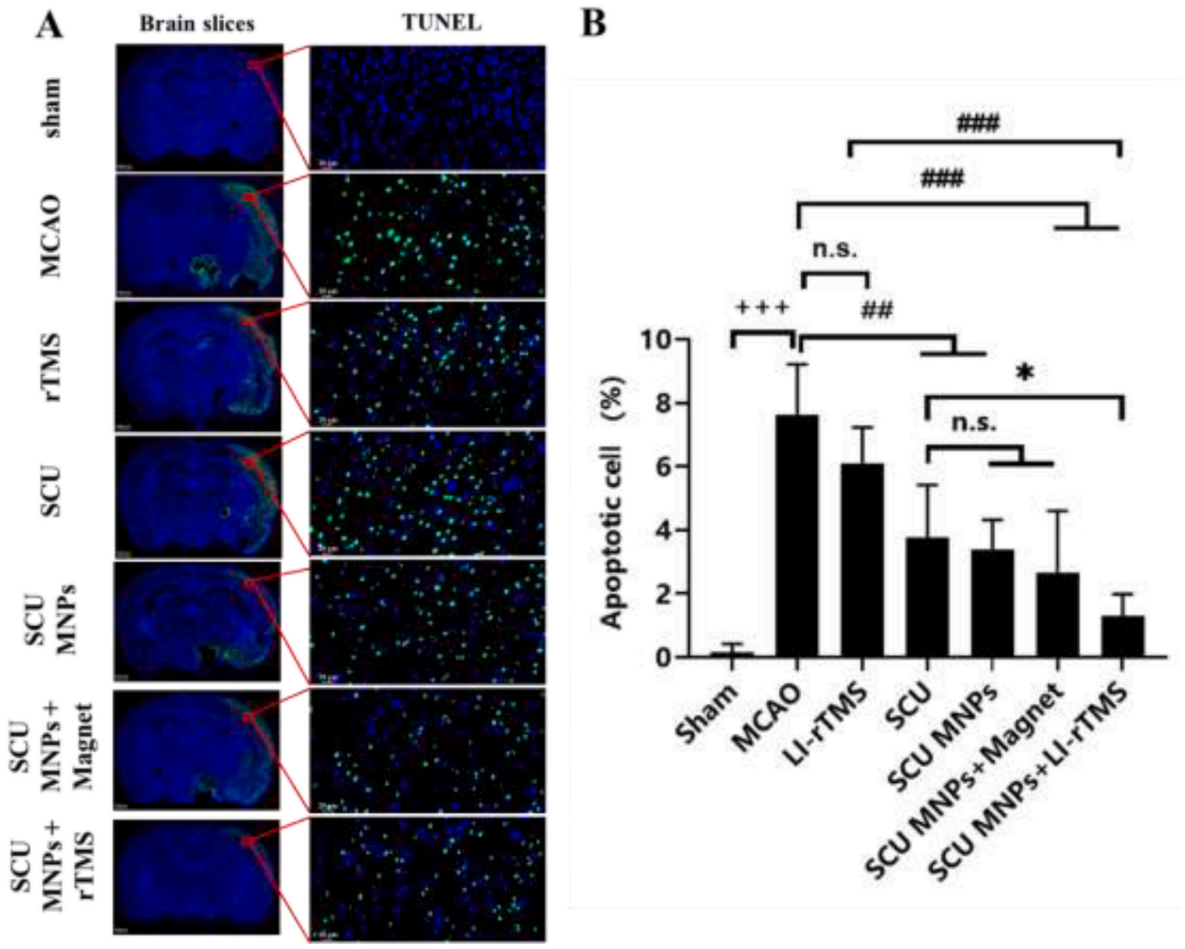

Fig. 10. Neuronal apoptosis of SCU MNPs under the magnetic field guidance. (A) Typical images of brain slices (scale bar: 1000 μm) and cells (scale bar: 20 μm) stained with TUNEL. DAPI was used to stain the nucleus (blue) and TUNEL was used to stain apoptotic cells (green). (B) The percentage of apoptotic cells in the brain of MCAO rats. SD rats were divided into the sham-operated (saline), MCAO (saline), LI-rTMS (saline), SCU, SCU MNPs, SCU MNPs + Magnet and SCU MNPs + LI-rTMS groups (n = 3). The apoptotic cells and total cells from the brain slices were quantified using Indica labs (Halo v3.0.311.314, USA). Data are presented as average ± SD. One-way analysis of variance (ANOVA) was used for the statistical analysis. + denotes comparison with sham group ($^{+}P < 0.05$, $^{++}P < 0.01$, $^{+++}P < 0.001$). $^{\#}$ denotes comparison with MCAO group ($^{\#}P < 0.05$, $^{\#\#}P < 0.01$, $^{\#\#\#}P < 0.001$). * denotes comparison with SCU group ($^{*}P < 0.05$, $^{**}P < 0.01$, $^{***}P < 0.001$).N.s. means not statistically significant. (For interpretation of the references to colour in this figure legend, the reader is referred to the Web version of this article.)

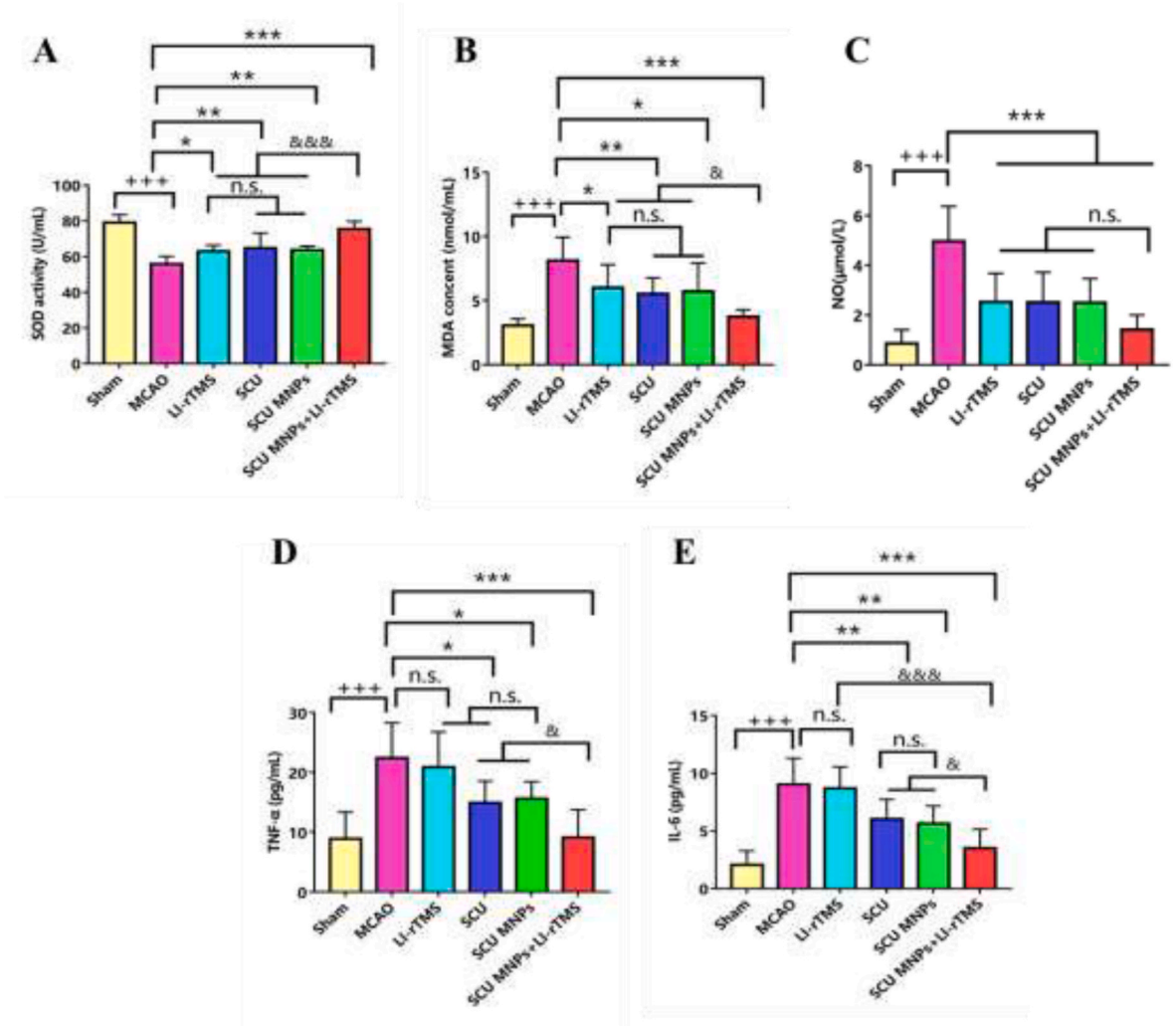

Fig. 11. SCU MNPs coupled with LI-rTMS reduced the oxidative stress and inflammation levels after ischemic stroke. (A) SOD activity in the serum. (B) MDA content in the serum. (C) NO content in the serum. (D) TNF-α level in the serum. (E) IL-6 level in the serum. Data were presented as the mean ± SD (n = 6). Statistical analysis was performed using one-way analysis of variance (ANOVA). + denotes comparison with sham group ($^{+++}P < 0.001$). * denotes comparison with MCAO group ($^{*}P < 0.05$, $^{**}P < 0.01$, $^{***}P < 0.001$). $^{\&}$ denotes comparison with SCU MNPs + LI-rTMS group ($^{\&}P < 0.05$, $^{\&\&\&}P < 0.001$). N.s. means not statistically significant.

stronger anti-oxidant activity from the change of SOD activity and MDA content, which suggests that SCU and LI-rTMS can exert synergistic therapeutic effects via anti-oxidant mechanisms. Unfortunately, in regard to NO level in the serum of MCAO rat, no significant difference was observed between treatment groups.

As shown in Fig. 11D and E, the serum TNF-α and IL-6 levels in the LI-rTMS group was similar to those in the MCAO group, which implies that LI-rTMS had no anti-inflammatory effect. Likewise, SCU and SCU MNPs groups had similar levels of TNF-α and IL-6, indicating that the anti-inflammation of SCU MNPs originated from SCU. Although the anti-inflammatory effect in the SCU MNPs + LI-rTMS group was stronger than that of SCU and SCU MNPs alone ($P < 0.05$), this may be due to the accumulation of SCU in the plasma and brain in the SCU MNPs + LI-rTMS group observed in Fig. 7.

4. Discussion

Throughout the world, stroke is one of the most common causes of disability and death [1–3]. The functional motor limitations that are present in between 55% and 75% of patients following a stroke episode influence their quality of life and ability to perform daily activities [41]. The use of physical therapy is essential in the recovery of motor skills [42]. rTMS is a painless and noninvasive brain stimulation technique that induces electromagnetic fields in the brain to modulate cortical excitability at the stimulation site and transsynaptically at distant locations [42,43]. As a result, rTMS has been used in stroke patients to rehabilitate limb motor function by stimulating the primary motor cortex (M1) [41,42]. Despite this, no significant benefit of our LI-rTMS was observed in the assessment of neurological behaviour for ischemia/reperfusion injury. Perhaps, the low intensity (6–9 mT) stimulation of neuronal systems may be insufficient to induce the electric field resulting in the treatment of neurological disorders [44–46]. However, LI-rTMS showed some anti-oxidant activity in Fig. 11A and B, which was consistent with the results reported by Medina-Fernández et al. [47]. The antioxidant effect of LI-rTMS may be the main reason for the synergistic mechanism with SCU against cerebral I/R injury.

SCU constitutes the majority of the active component (>90%) in breviscapine extracted from Erigeron breviscapus (Vant.) Hand.Mazz [48]. As a vasorelaxant, anticoagulant, anti-inflammatory, and anti-oxidant, it has been used by the Chinese for treating cerebral ischemic and cardiac ischemic diseases for centuries [37,38,48]. On the basis of research on network pharmacology, Meng et al. [49] identified NOS3 and F2 as scutellarin's key targets in the treatment of angina pectoris and ischemic stroke. Endothelial enzyme nitric oxide synthase (eNOS), encoded by the NOS3 gene, is a key enzyme responsible for nitric oxide (NO) generation in the vascular endothelium [50,51]. The

endothelial-derived NO signalling molecule has potent vasodilatory and anti-inflammatory properties known for protecting the vasculature [52]. Prothrombin (also known as coagulation factor II) is encoded by the F2 gene and is the precursor of thrombin, which plays a significant role in thrombus formation [53]. Hu et al. [54] and Liu et al. [55] discovered similar mechanisms behind SCU's brain-protective effects. As reported, our SCU and SCU MNPs had the brain protective effect against ischemia/reperfusion injury (Figss. 8–11). Promisingly, SCU MNPs increased SCU stability and extended its blood circulation and brain accumulation (Figs. 5 and 7). More importantly, SCU MNPs coupled with LI-rTMS can exert synergistic therapeutic effects against cerebral I/R injury through anti-oxidant and anti-inflammatory pathways (Fig. 11).

Over the last few decades, magnetic hyperthermia and drug delivery systems have been developed [26,56]. A static magnetic field based on magnets is primarily used in magnetic targeting drug delivery systems. Unfortunately, field strength rapidly diminishes with the depth of the target in the body. Relative focusing is possible using alternating magnetic fields [57]. The alternating magnetic field can penetrate biological tissue without much attenuation, thereby maintaining its intensity and stimulation consistency [26]. But the magnetic targeting strategy is not clear due to alternating magnetic field condition complex. Thus, alternating magnetic field was mainly used in the production of thermal to trigger drug release rather than the magnetic targeting.

This is, to the best of our knowledge, the first study in which SCU MNPs are combined with LI-rTMS to treat cerebral I/R injury. SCU MNPs under the exposure of magnet had no significant therapeutic efficacy against I/R injury except for cerebral infarct volume, even though the higher SCU level in MCAO rat brain was also observed at 4 h after administration of SCU MNPs (Fig. 7B). Surprisingly, SCU MNPs combination with the irradiation of LI-rTMS had more efficacies in the treatment of ischemic stroke compared with free SCU or SCU MNPs alone. There are perhaps three reasons behind this fact. The first reason is the improvement of SCU stability and the extension of SCU blood circulation as shown in Fig. 7 and Table 2. The second possible reason is the magnetic heating. Ischemic stroke was reported to result in the tight junction disruption and hyperpermeability of Blood Brain Barrier (BBB) [58–62]. The temperature elevation of MCAO rat head treated with SCU MNPs after the exposure of LI-rTMS perhaps enhances the permeability of BBB resulting in the increment of SCU in the brain recruited by the alternating magnetic field as shown in Figs. 6 and 7. The third possible synergistic reason was the anti-oxidant effect shown in Fig. 11. More interestingly, it is reported that low intensity of repetitive magnetic stimulation can modulate intracellular calcium levels in non-neuronal [63] and neuronal cells [64]. Additionally, another possible mechanism for the protective activity of SCU during ischemia reperfusion is an endothelium-independent vasorelaxant effect induced by the inhibition of extracellular calcium ions influx [38]. Unfortunately, the importance of intracellular calcium levels in the combination of SCU and LI-rTMS is still unclear. The exact mechanism behind the combination of LI-rTMS and SCU MNPs remains to be elucidated.

As a summary, our formulation can protect SCU from the complex biological environment such as pH and ions, thereby reducing the metabolic rate of SCU in the blood and brain. With the degradation of nanoparticles, SCU was gradually released to the circulation and the plasma concentration and brain level of drug can be sustained. Finally, the pharmacodynamic improvement was obtained by SCU MNPs under the exposure of AMF from LI-rTMS.

5. Conclusions

SCU and Fe_3O_4 nanoparticles were loaded into the PLGA NPs to obtain SCU MNPs using nanoprecipitation method. The prepared SCU MNPs were spherical and uniformly dispersed with small size and good encapsulation efficiency. *In-vitro* release experiments revealed the improvement of SCU stability by MNPs encapsulation. The AUC increase from pharmacokinetics implied the increase of SCU plasma concentration. The increase of half-life and mean retention time indicated the decrease of elimination rate and the extension of circulation time. The increase of SCU concentration in the brain by the MNPs encapsulation especially under the exposure of LI-rTMS was also observed in the brain distribution experiment. All the pharmacodynamic studies such as the TTC staining, HE staining, TUNEL staining, SOD and MDA test et al. investigated that the therapeutic efficacy of SCU MNPs combination with the LI-rTMS were better than the free SCU even SCU MNPs based on the rat MCAO model. Thus, it is safely concluded that the administration of SCU MNPs with the low-intensity magnetic stimulation would have a great potential to treat the ischemic cerebrovascular disease. The combination of magnetic nanoparticles and low-intensity magnetic stimulation also provides a promising tool for brain drug delivery system.

Funding

This work was supported by National Natural Science Foundation of China (grant number 81860323); the China Scholarship Council (contract 201808525113); Natural Science Foundation of Guizhou Province (grant number Qiankehejichu[2020]1Y401); Science and Technology Foundation of Guizhou Provincial Health Commission (grant number gzwjkj 2019-1-187); and High-level Talents Innovation and Entrepreneurship Merit-based Funding Projects of Guizhou Province [grant number (2021)03].

Author statement

Libin Wang: Methodology, Software, Investigation, Writing-original draft; Shanshan Yang: Methodology, Software, Investigation; Lisu Li: Visualization, Investigation; Yong Huang: Investigation; Ruixi Li: Visualization; Shumei Fang: Methodology, Investigation; Jincheng Jing: Methodology, Software; Chang Yang: Conceptualization, Supervision, Writing-reviewing & editing and Funding acquisition.

Declaration of competing interest

The authors declare that they have no known competing financial interests or personal relationships that could have appeared to influence the work reported in this paper.

Data availability

No data was used for the research described in the article.

Supplementary materials

Supplementary material associated with this article can be found, in the online version, at doi:.

Appendix A. Supplementary data

Supplementary data to this article can be found online at https://doi.org/10.1016/j.jddst.2022.103606.

References

[1] M. Katan, A. Luft, Global burden of stroke, Semin. Neurol. 38 (2018) 208–211, https://doi.org/10.5167/uzh-159894.

[2] E.J. Benjamin, P. Muntner, A. Alonso, M.S. Bittencourt, C.W. Callaway, A. P. Carson, A.M. Chamberlain, A.R. Chang, S. Cheng, S.R. Das, F.N. Delling, L. Djousse, M.S.V. Elkind, J.F. Ferguson, M. Fornage, L.C. Jordan, S.S. Khan, B. M. Kissela, K.L. Knutson, T.W. Kwan, D.T. Lackland, T.T. Lewis, J.H. Lichtman, C. T. Longenecker, M.S. Loop, P.L. Lutsey, S.S. Martin, K. Matsushita, A.E. Moran, M. E. Mussolino, M. O'Flaherty, A. Pandey, A.M. Perak, W.D. Rosamond, G.A. Roth, U. K.A. Sampson, G.M. Satou, E.B. Schroeder, S.H. Shah, N.L. Spartano, A. Stokes, D. L. Tirschwell, C.W. Tsao, M.P. Turakhia, L.B. VanWagner, J.T. Wilkins, S.S. Wong, S.S. Virani, On behalf of the American heart association Council on epidemiology

and prevention statistics committee and stroke statistics subcommittee, heart disease and stroke statistics-2019 update: a report from the American heart association, Circulation 139 (2019) e56–e528, https://doi.org/10.1161/CIR.0000000000000659.
[3] J.D. Spence, China Stroke Statistics 2019: a wealth of opportunities for stroke prevention, Stroke Vasc. Neurol. 5 (2020) 240–241, https://doi.org/10.1136/svn-2020-000529.
[4] S. Paul, E. Candelario-Jalil, Emerging neuroprotective strategies for the treatment of ischemic stroke: an overview of clinical and preclinical studies, Exp. Neurol. 335 (2021), 113518, https://doi.org/10.1016/j.expneurol.2020.113518.
[5] T. Leng, Z. Xiong, Treatment for ischemic stroke: from thrombolysis to thrombectomy and remaining challenges, Brain Circ 5 (2019) 8–11, https://doi.org/10.4103/bc.bc_36_18.
[6] P. Jolugbo, R.A.S. Ariëns, Thrombus composition and efficacy of thrombolysis and thrombectomy in acute ischaemic stroke, Stroke 52 (2021) 1131–1142, https://doi.org/10.1161/STROKEAHA.120.032810.
[7] W. Klomjai, R. Katz, A. Lackmy-Vallée, Basic principles of transcranial magnetic stimulation (TMS) and repetitive TMS (rTMS), Ann. Phys. Rehabil. Med. 58 (2015) 208–213, https://doi.org/10.1016/j.rehab.2015.05.005.
[8] A.R. Chaves, N.J. Snow, L.R. Alcock, M. Ploughman, Probing the brain–body connection using transcranial magnetic stimulation (TMS): validating a promising tool to provide biomarkers of neuroplasticity and central nervous system function, Brain Sci. 11 (2021) 384, https://doi.org/10.3390/brainsci11030384.
[9] J.P. Lefaucheur, A. Aleman, C. Baeken, D.H. Benninger, J. Brunelin, V. Di Lazzaro, S.R. Filipović, C. Grefkes, A. Hasan, F.C. Hummel, S.K. Jääskeläinen, B. Langguth, L. Leocani, A. Londero, R. Nardone, J.P. Nguyen, T. Nyffeler, A.J. Oliveira-Maia, A. Oliviero, F. Padberg, U. Palm, W. Paulus, E. Poulet, A. Quartarone, F. Rachid, I. Rektorová, S. Rossi, H. Sahlsten, M. Schecklmann, D. Szekely, U. Ziemann, Evidence-based guidelines on the therapeutic use of repetitive transcranial magnetic stimulation (rTMS): an update (2014–2018), Clin. Neurophysiol. 131 (2020) 474–528, https://doi.org/10.1016/j.clinph.2019.11.002.
[10] X. Moisset, D. Bouhassira, N. Attal, French guidelines for neuropathic pain: an update and commentary, Rev. Neurol. (Paris) 177 (2021) 834–837, https://doi.org/10.1016/j.neurol.2021.07.004.
[11] F. Fisicaro, G. Lanza, A.A. Grasso, G. Pennisi, R. Bella, W. Paulus, M. Pennisi, Repetitive transcranial magnetic stimulation in stroke rehabilitation: review of the current evidence and pitfalls, Ther. Adv. Neurol. Disord. 12 (2019) 1–22, https://doi.org/10.1177/1756286419878317.
[12] S. Rossi, A. Antal, S. Bestmann, M. Bikson, C. Brewer, J. Brockmöller, L. L. Carpenter, M. Cincotta, R. Chen, J.D. Daskalakis, V.D. Lazzaro, M.D. Fox, M. S. George, D. Gilbert, V.K. Kimiskidis, G. Koch, R.J. Ilmoniemi, J.P. Lefaucheur, L. Leocani, S.H. Lisanby, C. Miniussi, F. Padberg, A. Pascual-Leone, W. Paulus, A. V. Peterchev, A. Quartarone, A. Rotenberg, J. Rothwell, P.M. Rossini, E. Santarnecchi, M.M. Shafi, H.R. Siebner, Y. Ugawa, E.M. Wassermann, A. Zangen, U. Ziemann, M. Hallett, Safety and recommendations for TMS use in healthy subjects and patient populations, with updates on training, ethical and regulatory issues: expert Guidelines, Clin, Neurophysiology 132 (2021) 269–306, https://doi.org/10.1016/j.clinph.2020.10.003.
[13] P. Zis, F. Shafique, M. Hadjivassiliou, D. Blackburn, A. Venneri, S. Iliodromiti, D. D. Mitsikostas, P.G. Sarrigiannis, Safety, tolerability, and nocebo phenomena during transcranial magnetic stimulation: a systematic review and meta-analysis of placebo-controlled clinical trials, Neuromodulation 23 (2020) 291–300, https://doi.org/10.1111/ner.12946.
[14] D.J. Stultz, S. Osburn, T. Burns, S. Pawlowska-Wajswol, R. Walton, Transcranial magnetic stimulation (TMS) safety with respect to seizures: a literature review, Neuropsychiatric Dis. Treat. 16 (2020) 2989–3000, https://doi.org/10.2147/NDT.S276635.
[15] L. Wang, Q. Zhao, S. Yang, T. Liu, C. Yang, Study on the neuroprotective effect of scutellarin based on rat middle cerebral artery occlusion model, Guizhou Med. 45 (2021) 1347–1350, 09.
[16] J. Lu, C. Cheng, X. Zhao, Q. Liu, P. Yang, Y. Wang, G. Luo, PEG-scutellarin prodrugs: synthesis, water solubility and protective effect on cerebral ischemia/reperfusion injury, Eur. J. Med. Chem. 45 (2010) 1731–1738, https://doi.org/10.1016/j.ejmech.2010.01.006.
[17] Y. Wei, L. Li, Y. Xi, S. Qian, Y. Gao, J. Zhang, Sustained release and enhanced bioavailability of injectable scutellain-loaded bovine serum albumin nanoparticles, Int. J. Pharm. 476 (2014) 142–148, https://doi.org/10.1016/j.ijpharm.2014.09.038.
[18] Z. Liu, C.I. Okeke, L. Zhang, H. Zhao, J. Li, M.O. Aggrey, N. Li, X. Guo, X. Pang, L. Fan, L. Guo, Mixed polyethylene glycol-modified breviscapine-loaded solid lipid nanoparticles for improved brain bioavailability: preparation, characterization, and *in vivo* cerebral microdialysis evaluation in adult Sprague Dawley rats, AAPS PharmSciTech 15 (2014) 483–496, https://doi.org/10.1208/s12249-014-0080-4.
[19] C. Yang, Q. Zhao, S. Yang, L. Wang, X. Xu, L. Li, W.T. Al-Jamal, Intravenous administration of scutellarin nanoparticles augments the protective effect against the cerebral ischemia-reperfusion injury in rats, Mol. Pharm. 19 (2022) 1410–1421, https://doi.org/10.1021/acs.molpharmaceut.1c00942.
[20] W. Huang, C. Zhang, Tuning the size of poly(lactic-co-glycolic acid) (PLGA) nanoparticles facricated by nanoprecipitation, Biotechnol. J. 13 (2018), 1700203, https://doi.org/10.1002/biot.201700203.
[21] J. Ghitman, R. Stan, A. Ghebaur, S. Cecoltan, E. Vasile, H. Iovu, Novel PEG-modified hybrid PLGA-vegetable oils nanostructured carriers for improving performances of indomethacin delivery, Polymers 10 (2018) 579, https://doi.org/10.3390/polym10060579.
[22] E.Z. Longa, P.R. Weinstein, S. Carlson, R. Cummins, Reversible middle cerebral artery occlusion without craniectomy in rats, Stroke 20 (1989) 84–91, https://doi.org/10.1161/01.str.20.1.84.
[23] S. Ansari, H. Azari, D.J. McConnell, A. Afzal, J. Mocco, Intraluminal middle cerebral artery occlusion (MCAO) model for ischemic stroke with laser Doppler flowmetry guidance in mice, JoVE 51 (2011) 2879, https://doi.org/10.3791/2879.
[24] C. Wang, H. Chen, H.H. Jiang, B.B. Mao, H. Yu, Total flavonoids of Chuju decrease oxidative stress and cell apoptosis in ischemic stroke rats: network and experimental analyses, Front. Neurosci. 15 (2021), 772401, https://doi.org/10.3389/fnins.2021.772401.
[25] S. Chen, M. Li, Y. Li, H. Hu, Y. Li, Y. Huang, L. Zheng, Y. Lu, J. Hu, Y. Lan, A. Wang, Y. Li, Z. Gong, Y. Wang, A UPLC-ESI-MS/MS method for simultaneous quantitation of chlorogenic Acid, scutellarin, and scutellarein in rat plasma: application to a comparative pharmacokinetic study in sham-operated and MCAO rats after oral administration of Erigeron breviscapus extract, Molecules 23 (2018) 1808, https://doi.org/10.3390/molecules23071808.
[26] F. D'Agata, F.A. Ruffinatti, S. Boschi, I. Stura, I. Rainero, O. Abollino, R. Cavalli, C. Guiot, Magnetic nanoparticles in the central nervous system: targeting principles, applications and safety issues, Molecules 23 (2017) 9, https://doi.org/10.3390/molecules23010009.
[27] Y. Xu, C. Kim, D. Saylor, D. Koo, Polymer degradation and drug delivery in PLGA based drug-polymer applications: a review of experiments and theories, J. Biomed. Mater. Res. Part B Appl. Biomater. 105 (2017) 1692–1716, https://doi.org/10.1002/jbm.b.33648.
[28] H.K. Makadia, S.J. Siegel, Poly lactic-co-glycolic acid (PLGA) as biodegradable controlled drug delivery carrier, Polymers 3 (2011) 1377–1397, https://doi.org/10.3390/polym3031377.
[29] L.P. Jahromi, M. Ghazali, H. Ashrafi, A. Azadi, A comparison of models for the analysis of the kinetics of drug release from PLGA-based nanoparticles, Heliyon 6 (2020), e03451, https://doi.org/10.1016/j.heliyon.2020.e03451.
[30] J. Wu, S. Xu, C.C. Han, G. Yuan, Controlled drug release: on the evolution of physically entrapped drug inside the electrospun poly(lactic-co-glycolic acid) matrix, J. Contr. Release 331 (2021) 472–479, https://doi.org/10.1016/j.jconrel.2021.01.038.
[31] P. Das, M. Colombo, D. Prosperi, Recent advances in magnetic fluid hyperthermia for cancer therapy, Colloids Surf. B Biointerfaces 174 (2019) 42–55, https://doi.org/10.1016/j.colsurfb.2018.10.051.
[32] V. Vilas-Boas, F. Carvalho, B. Espiña, Magnetic hyperthermia for cancer treatment: main parameters affecting the outcome of in vitro and in vivo studies, Molecules 25 (2020) 2874, https://doi.org/10.3390/molecules25122874.
[33] H. Gavilán, S.K. Avugadda, T. Fernández-Cabada, N. Soni, M. Cassani, B.T. Mai, R. Chantrell, T. Pellegrino, Magnetic nanoparticles and clusters for magnetic hyperthermia: optimizing their heat performance and developing combinatorial therapies to tackle cancer, Chem. Soc. Rev. 50 (2021) 11614–11667, https://doi.org/10.1039/D1CS00427A.
[34] P. Chandrasekharan, Z.W. Tay, D. Hensley, X.Y. Zhou, B.K. Fung, C. Colson, Y. Lu, B.D. Fellows, Q. Huynh, C. Saayujya, E. Yu, R. Orendorff, B. Zheng, P. Goodwill, C. Rinaldi, S. Conolly, Using magnetic particle imaging systems to localize and guide magnetic hyperthermia treatment: tracers, hardware, and future medical applications, Theranostics 10 (2020) 2965–2981, https://doi.org/10.7150/thno.40858.
[35] R. Peyron, C. Fauchon, Functional imaging of pain, Rev, Neurol. 175 (2019) 38–45, https://doi.org/10.1016/j.neurol.2018.08.006.
[36] N. Eimantas, S. Ivanove, R. Solianik, M. Brazaitis, Exposure to acute noxious heat evokes a cardiorespiratory shock response in humans, Int. J. Hyperther. 39 (2022) 134–143, https://doi.org/10.1080/02656736.2021.2023225.
[37] J. Gao, G. Chen, H. He, C. Liu, X. Xiong, J. Li, J. Wang, Therapeutic effects of breviscapine in cardiovascular diseases: a review, Front. Pharmacol. 8 (2017) 289, https://doi.org/10.3389/fphar.2017.00289.
[38] S. Chledzik, J. Strawa, K. Matuszek, J. Nazaruk, Pharmacological effects of scutellarin, an active component of genus *Scutellaria* and *Erigeron*: a systematic review, Am. J. Chin. Med. 46 (2018) 319–337, https://doi.org/10.1142/S0192415X18500167.
[39] C. Saraiva, C. Praça, R. Ferreira, T. Santos, L. Ferreira, L. Bernardino, Nanoparticle-mediated brain drug delivery: overcoming blood–brain barrier to treat neurodegenerative diseases, J. Contr. Release 235 (2016) 34–47, https://doi.org/10.1016/j.jconrel.2016.05.044.
[40] Y. Fu, R. Xing, L. Wang, L. Yang, B. Jiang, Neurovascular protection of salvianolic acid B and ginsenoside Rg1 combination against acute ischemic stroke in rats, Neuroreport 32 (2021) 1140–1146, https://doi.org/10.1097/WNR.0000000000001706.
[41] A. Dionísio, I.C. Duarte, M. Patrício, M. Castelo-Branco, The use of repetitive transcranial magnetic stimulation for stroke rehabilitation: a systematic review, J. Stroke Cerebrovasc. Dis. 27 (2018) 1–31, https://doi.org/10.1016/j.jstrokecerebrovasdis.2017.09.008.
[42] S.C.B. Galvão, R.B.C. dos Santos, P.B. dos Santos, M.E. Cabral, K. Monte-Silva, Efficacy of coupling repetitive transcranial magnetic stimulation and physical therapy to reduce upper-limb spasticity in patients with stroke: a randomized controlled trial, Arch. Phys. Med. Rehabil. 95 (2014) 222–229, https://doi.org/10.1016/j.apmr.2013.10.023.
[43] Y. Terao, Y. Ugawa, Basic mechanisms of TMS, J. Clin. Neurophysiol. 19 (2002) 322–343, https://doi.org/10.1097/00004691-200208000-00006.
[44] D. Rudiak, E. Marg, Finding the depth of magnetic brain stimulation: a re-evaluation, Electroencephalogr. Clin. Neurophysiol. 93 (1994) 358–371, https://doi.org/10.1016/0168-5597(94)90124-4.

[45] K.R. Davey, M. Riehl, Suppressing the surface field during transcranial mag- netic stimulation, IEEE Trans. Biomed. Eng. 53 (2006) 190–194, https://doi.org/10.1109/TBME.2005.862545.
[46] Z. Turi, M. Lenz, W. Paulus, M. Mittner, A. Vlachos, Selecting stimulation intensity in repetitive transcranial magnetic stimulation studies: a systematic review between 1991 and 2020, Eur. J. Neurosci. 53 (2021) 3404–3415, https://doi.org/10.1111/ejn.15195.
[47] F.J. Medina-Fernández, B.M. Escribano, C. Padilla-Del-Campo, R. Drucker-Colín, Á. Pascual-Leone, I. Túnez, Transcranial magnetic stimulation as an antioxidant, Free Radic. Res. 52 (2018) 381–389, https://doi.org/10.1080/10715762.2018.1434313.
[48] L. Wang, Q. Ma, Clinical benefits and pharmacology of scutellarin: a comprehensive review, Pharmacol. Ther. 190 (2018) 105–127, https://doi.org/10.1016/j.pharmthera.2018.05.006.
[49] Z.Q. Meng, J.R. Wu, Y.L. Zhu, W. Zhou, C.G. Fu, X.K. Liu, S.Y. Liu, M.W. Ni, S. Y. Guo, Revealing the common mechanisms of scutellarin in angina pectoris and ischemic stroke treatment via a network pharmacology approach, Chin. J. Integr. Med. 27 (2021) 62–69, https://doi.org/10.1007/s11655-020-2716-4.
[50] B.A. Nassar, L.D. Bevin, D.E. Johnstone, B.J. O'neill, I.R. Bata, S.A. Kirkland, L. M. Title, Relationship of the Glu298Asp polymorphism of the endothelial nitric oxide synthase gene and early-onset coronary artery disease, Am. Heart J. 142 (2001) 586–589, https://doi.org/10.1067/mhj.2001.118113.
[51] M.R. Luizon, D.A. Pereira, J.E. Tanus-Santos, Pharmacogenetic relevance of endothelial nitric oxide synthase polymorphisms and gene interactions, Pharmacogenomics 19 (2018) 1423–1435, https://doi.org/10.2217/pgs-2018-0098.
[52] A.R. Cyr, L.V. Huckaby, S.S. Shiva, B.S. Zuckerbraun, Nitric oxide and endothelial dysfunction, Crit. Care Clin. 36 (2020) 307–321, https://doi.org/10.1016/j.ccc.2019.12.009.
[53] M. Chinnaraj, W. Planer, N. Pozzi, Structure of coagulation factor II:molecular mechanism of thrombin generation and development of next-generation anticoagulants, Front. Med. 5 (2018) 281, https://doi.org/10.3389/fmed.2018.00281.
[54] X.M. Hu, M.M. Zhou, X.M. Hu, F.D. Zeng, Neuroprotective effects of scutellarin on rat neuronal damage induced by cerebral ischemia/reperfusion, Acta Pharmacol. Sin. 12 (2005) 1454–1459, https://doi.org/10.1111/j.1745-7254.2005.00239.x.
[55] G. Liu, Y. Liang, M. Xu, M. Sun, W. Sun, Y. Zhou, X. Huang, W. Song, Y. Liang, Z. Wang, Protective mechanism of Erigeron breviscapus injection on blood-brain barrier injury induced by cerebral ischemia in rats, Sci. Rep. 11 (2021), 18451, https://doi.org/10.1038/s41598-021-97908-x.
[56] S.M. Dadfar, K. Roemhild, N.I. Drude, S. von Stillfried, R. Knüchel, F. Kiessling, T. Lammers, Iron oxide nanoparticles: diagnostic, therapeutic and theranostic applications, Adv. Drug Deliv. Rev. 138 (2019) 302–325, https://doi.org/10.1016/j.addr.2019.01.005.
[57] B. Shapiro, S. Kulkarni, A. Nacev, S. Muro, P.Y. Stepanov, I.N. Weinberg, Open challenges in magnetic drug targeting, Wiley Interdiscip. Rev. Nanomed. Nanobiotechnol. 7 (2015) 446–457, https://doi.org/10.1002/wnan.1311.
[58] D. Knowland, A. Arac, K.J. Sekiguchi, M. Hsu, S.E. Lutz, J. Perrino, G.K. Steinberg, B.A. Barres, A. Nimmerjahn, D. Agalliu, Stepwise recruitment of transcellular and paracellular pathways underlies blood-brain barrier breakdown in stroke, Neuron 82 (2014) 603–617, https://doi.org/10.1016/j.neuron.2014.03.003.
[59] G.A. Rosenberg, Y. Yang, Vasogenic edema due to tight junction disruption by matrix metalloproteinases in verebral ischemia, Neurosurg. Focus 22 (2007) E4, https://doi.org/10.3171/foc.2007.22.5.5.
[60] S.E. Lakhan, A. Kirchgessner, D. Tepper, A. Leonard, Matrix metalloproteinases and blood-brain barrier disruption in acute ischemic stroke, Front. Neurol. 4 (2013) 32, https://doi.org/10.3389/fneur.2013.00032.
[61] K. Arai, J. Lok, S. Guo, K. Hayakawa, C. Xing, E.H. Lo, Cellular mechanisms of neurovascular damage and repair after stroke, J. Child Neurol. 26 (2011) 1193–1198, https://doi.org/10.1177/0883073811408610.
[62] Z.S. Al-Ahmady, D. Jasim, S.S. Ahmad, R. Wong, M. Haley, G. Coutts, I. Schiessl, S. M. Allan, K. Kostarelos, Selective liposomal transport through blood brain barrier disruption in ischemic stroke reveals two distinct therapeutic opportunities, ACS Nano 13 (2019) 12470–12486, https://doi.org/10.1021/acsnano.9b01808.
[63] X. Zhang, X. Liu, L. Pan, I. Lee, Magnetic fields at extremely low-frequency (50 Hz, 0.8 mT) can induce the uptake of intracellular calcium levels in osteoblasts, Biochem. Biophys. Res. Commun. 396 (2010) 662–666, https://doi.org/10.1016/j.bbrc.2010.04.154.
[64] S. Grehl, H.M. Viola, P.I. Fuller-Carter, K.W. Carter, S.A. Dunlop, L.C. Hool, R. M. Sherrard, J. Rodger, Cellular and molecular changes to cortical neurons following low intensity repetitive magnetic stimulation at different frequencies, Brain Stimul. 8 (2015) 114–123, https://doi.org/10.1016/j.brs.2014.09.012.